ApJ, submitted 11/17/2006
Preprint typeset using LaTeX style emulateapj v. 10/09/06

DYNAMICAL MODELS OF ELLIPTICAL GALAXIES IN $Z = 0.5$ CLUSTERS: II. MASS-TO-LIGHT RATIO EVOLUTION WITHOUT FUNDAMENTAL PLANE ASSUMPTIONS

Roeland P. van der Marel
Space Telescope Science Institute, 3700 San Martin Drive, Baltimore, MD 21218

Pieter G. van Dokkum
Department of Astronomy, Yale University, New Haven, CT 06520
ApJ, submitted 11/17/2006

ABSTRACT

We study M/L evolution of early-type galaxies using dynamical modeling of resolved internal kinematics. This makes fewer assumptions than Fundamental Plane (FP) studies and provides a powerful new approach for studying galaxy evolution. We focus on the sample of 25 galaxies in clusters at $z \approx 0.5$ modeled in Paper I. For comparison we compile and homogenize M/L literature data for 60 nearby galaxies that were modeled in comparable detail. The nearby sample obeys $\log(M/L)_B = Z + S\log(\sigma_{\rm eff}/[200\,{\rm km\,s^{-1}}])$, with $Z = 0.896 \pm 0.010$, $S = 0.992 \pm 0.054$, and $\sigma_{\rm eff}$ the effective velocity dispersion. The $z \approx 0.5$ sample follows a similar relation but with lower zeropoint. The implied M/L evolution is $\Delta\log(M/L)/\Delta z = -0.457 \pm 0.046\,({\rm random}) \pm 0.078\,({\rm systematic})$, consistent with passive evolution following high-redshift formation. This agrees with the FP results for this sample by van Dokkum & van der Marel. This confirms that FP evolution tracks M/L evolution, which is an important verification of the assumptions that underly FP studies. However, while we find more FP evolution for galaxies of low $\sigma_{\rm eff}$ (or low mass), the dynamical M/L evolution instead shows little trend with $\sigma_{\rm eff}$. We argue that this difference can be plausibly attributed to a combination of two effects: (a) evolution in structural galaxy properties other than M/L; and (b) the neglect of rotational support in studies of FP evolution. The results leave the question open whether the low-mass galaxies in the sample have younger population ages than the high-mass galaxies. This highlights the general importance in the study of population ages for complementing dynamical measurements with broad-band colors or spectroscopic population diagnostics.

Subject headings: galaxies: clusters: individual (CL3C295, CL0016+16, CL1601+42) — galaxies: evolution — galaxies: formation — galaxies: kinematics and dynamics.

1. INTRODUCTION

A stellar population of fixed mass fades as it ages. The predicted mass-to-light ratio M/L of a galaxy therefore depends strongly on its age (e.g., Bruzual & Charlot 2003) and M/L measurements can constrain galaxy formation times. The M/L of a galaxy cannot generally be accurately constrained from characteristics of the observed light (e.g., broad-band colors and line-strength indices) alone. This is because low-mass stars contribute the bulk of the mass, but only a small fraction of the light. Plausible variations in the assumed initial mass function (IMF) can therefore change the M/L without affecting significantly the characteristics of the observed light (e.g., Bell & de Jong 2001). Accurate measurements of galaxy M/L values therefore generally rely on dynamical properties. The speed at which stars or gas move probes directly the gravitational force to which they are subjected, and therefore the mass of the system.

The quality of the kinematical data for galaxies in the local Universe, as well as the methods by which their dynamics can be modeled, have steadily increased in sophistication over the years. Large samples of reliable M/L measurements are now available from many studies, in particular for early-type galaxies (e.g., van der Marel 1991; Magorrian et al. 1998; Gebhardt et al. 2003; Cappellari et al. 2006a). For these galaxies it is well established that the M/L inside an effective radius is relatively constant, and contains only a small contribution from the dark halo (e.g., Kronawitter et al. 2000). Therefore, the inferred M/L values are primarily driven by the characteristics of the stellar population. This situation differs considerably from the case for spiral galaxies. While mass profiles have been derived for many spiral galaxies (e.g., Persic, Salucci & Stel 1996), these profiles constrain primarily the properties of the dark halo. Considerable uncertainty remains on the M/L of the stellar population, or alternatively, on whether spiral galaxy disks are "maximal" or not (e.g., van Albada et al. 1985; Courteau & Rix 1999).

Uncertainties in the IMF for low-mass stars cause considerable uncertainty in the predicted M/L at fixed age. So while accurate dynamical M/L measurements are available for many early-type galaxies, these do not uniquely constrain the age of their stellar population. A more powerful constraint is provided by the *relative* rate at which the M/L varies with time, or alternatively, redshift: $[d(M/L)/(M/L)]/dz \propto d\log(M/L)/dz$. Because this is a relative measure, it depends less strongly on uncertainties in the IMF for low-mass stars. Of course, a dependence does remain on the exact shape of the IMF for the higher-mass stars that produce most of the light. Nonetheless, $d\log(M/L)/dz$ can be used to meaningfully constrain the formation redshift of early-type galaxies (van Dokkum et al. 1998).

Studies of $d\log(M/L)/dz$ have so far relied primar-

ily on measurements of the Fundamental Plane (FP) for galaxies in the nearby and distant Universe (van Dokkum & Franx 1996). The FP is a tight planar relation between the global properties of early-type galaxies in any three-dimensional parameter space spanned by quantities that measure the characteristic galaxy size, velocity dispersion, and surface brightness (Djorgovski & Davis 1987; Dressler et al. 1987). For example, one might take the effective radius $r_{\rm eff}$, the average velocity dispersion $\sigma_{\rm eff}$ inside the effective radius, and the average surface brightness $I_{\rm eff}$ inside the effective radius. The existence of the FP can be understood as a combination of the virial theorem and a power-law dependence of M/L on global galaxy properties (Dressler et al. 1987; Cappellari et al. 2006a). A decrease in M/L with redshift due to stellar population effects corresponds to an increase in $I_{\rm eff}$, and consequently, a measurable decrease in the zeropoint of the FP.

Studies of FP evolution have provided important new insights into the formation and evolution of early-type galaxies (see, e.g., the following recent papers and references therein: Wuyts et al. 2004; Woo et al. 2004; Moran et al. 2005; Treu et al. 2005a,b; van der Wel et al. 2004, 2005; di Serego Alighieri et al. 2005; Jorgensen et al. 2006). In van Dokkum & van der Marel (2006, hereafter vDvdM06), we presented spectroscopy with the Low Resolution Imager and Spectrograph (LRIS) on Keck of some two dozen galaxies in the intermediate-redshift ($z \approx 0.5$) clusters CL3C295, CL0016+16 and CL1601+42. The sample galaxies were selected to be bright enough for spectroscopy, and visually classified from the Hubble Space Telescope (HST) images of Dressler et al. (1997) and Smail et al. (1997) as early-type (and in most cases elliptical) galaxies. We measured the integrated velocity dispersions of the galaxies and analyzed existing HST images to infer their characteristic photometric properties. This allowed a study of the FP evolution of the three sample clusters. We combined our new results with existing FP data for eleven additional clusters in the redshift range $0.18 \leq z \leq 1.28$ as well as samples of field early-type galaxies in the redshift range $0.32 \leq z \leq 1.14$. This provides the largest homogenized analysis of FP evolution to date and implies a luminosity-weighted mean star formation redshift $z_* = 2.01^{+0.22}_{-0.17}$ for massive ($M > 10^{11}\,{\rm M}_\odot$) early-type galaxies in clusters. Field early-type galaxies in the same mass range are only $4.1 \pm 2.0\%$ younger, with $z_* = 1.95^{+0.10}_{-0.08}$. (These results assume that the IMF has a "standard" form and that the progenitor bias described by van Dokkum & Franx (2001) does not depend on environment; see vDvdM06 for details).

The success and popularity of FP studies can be attributed at least in part to the relative ease with which such studies can be performed. Only global galaxy properties need to be measured, and modeling of the internal structure of the sample galaxies is not required. However, there are important caveats. In particular, values of $d\log(M/L)/dz$ determined from FP evolution are correct only if many simplifying assumptions are satisfied. Any potential evolution of global galaxy properties other than M/L (i.e., $\sigma_{\rm eff}$, $r_{\rm eff}$ and $\Sigma_{\rm eff} \equiv (M/L) \times I_{\rm eff}(r)$, the latter quantity being the average projected surface mass density inside $r_{\rm eff}$) must either be absent or be such so as to not affect the inferred M/L evolution. Also, galaxies must change homologously with redshift, if at all; they must not evolve in quantities such as the shape of their three-dimensional contours, the shape of their density profile with radius, or the shape of their intrinsic dynamical structure. The possibility that evolution in any of these quantities may in fact occur has left the interpretation of FP studies somewhat uncertain. This possibility has come into sharp focus through the fact that the inferred M/L evolution of massive early-type galaxies is well fit by models of passive evolution following formation at high redshift, and by the fact that there appears to be only a small age difference between massive early-type galaxies in clusters and the field (vDvdM06). Although models can be constructed that reproduce these results (e.g., Nagamine et al. 2005; De Lucia et al. 2006), they do appear somewhat counter-intuitive given the paradigm of hierarchical structure formation in the Universe. Moreover, there exist sophisticated semi-analytical models in which the evolution of galaxy M/L and FP zeropoint are actually quite different (Almeida, Baugh & Lacey 2006). So there are many reasons to critically question whether FP evolution does in fact uniquely trace M/L evolution.

The most direct way to address this question is to determine M/L values for individual distant galaxies in the same way as has been done locally, without resorting to FP assumptions. This requires construction of detailed dynamical models for high-quality spatially resolved photometric and kinematic data. With these goals in mind we obtained spectroscopic data in vDvdM06 that was deep enough to extract spatially resolved rotation curves and velocity dispersion profiles for the sample galaxies in CL3C295, CL0016+16 and CL1601+42. In van der Marel & van Dokkum (2006, hereafter Paper I) we presented the kinematical profiles and constructed detailed dynamical models to interpret them. The models are axisymmetric and are based on solving the Jeans equations of hydrostatic equilibrium under the assumption of a two-integral distribution function $f = f(E, L_z)$, where E is the energy and L_z the angular momentum around the symmetry axis. Fitting of the models to the available HST imaging and observed kinematical profiles yields two quantities: a normalized measure k of the galaxy's rotation rate and the M/L of the stellar population (in rest-frame B band solar units). The inferred values for these quantities and their formal uncertainties were presented in Paper I. The implications of the inferred rotation rates were also discussed in that paper. In the present paper we interpret the inferred M/L values. To do this, we first compile and homogenize a comparison sample of galaxies in the local Universe with reliable M/L determinations from the literature. We then compare the M/L values for the intermediate-redshift cluster galaxies to those for the local comparison sample to obtain a direct measure of the M/L evolution of elliptical galaxies.

The layout of this paper is as follows. Section 2 discusses the compilation of the local comparison sample of galaxies with dynamically inferred M/L values. Section 3 compares the M/L values for the galaxies in the intermediate-redshift sample from Paper I to those from the local compilation. This yields $d\log(M/L)/dz$, which is compared to the FP evolution of the same sample derived in vDvdM06. Section 4 discusses how the M/L evo-

TABLE 1
Sources of systematic uncertainty that affect $\log(M/L)$ measurements

ID	$\Delta \log(M/L)$	source of systematic uncertainty	Section
I	± 0.003	effect of uncertainties in $\Omega_{\rm m}$ and Ω_Λ at $z \approx 0.5$	1
II	± 0.026	accuracy with which the SBF and Cepheid distance scales have been aligned	2.2
III	± 0.037	accuracy of the Cepheid distance scale for local galaxies	2.2
IV	± 0.009	cosmic variance in H_0 on the scale $z \lesssim 0.1$	2.2
V	± 0.023	random uncertainty in H_0 due to finite sample sizes	2.2
VI	± 0.020	difference in results from different dynamical modeling approaches	2.5

Note. — Column (1) lists the roman numeral with which a particular systematic uncertainty is referred to in the text. Column (2) lists the size of the systematic uncertainty. Column (3) lists the source of the systematic uncertainty. Column (4) lists the number of the section in which the uncertainty is discussed.

lution depends on galaxy dispersion (or similarly mass), both in the present study and in the FP analysis. The uncertainties in both methods are discussed, as well as the implications for the accuracies of the inferred M/L evolution. Section 5 presents a summary and discussion of the results.

The dynamically inferred M/L of a galaxy is inversely proportional to the assumed distance. Throughout this paper (as in Paper I) we assume a cosmology with $\Omega_{\rm m} = 0.27$, $\Omega_\Lambda = 0.73$ (the values obtained by the Wilkinson Microwave Anisotropy Probe; Spergel et al. 2003) and $H_0 = 71\,{\rm km\,s^{-1}\,Mpc^{-1}}$ (the value obtained by the HST Cepheid Key Project; Section 7 of Freedman et al. 2001). The uncertainties in $\Omega_{\rm m}$, Ω_Λ can be estimated to be ~ 0.02 (Spergel et al. 2003). At $z \approx 0.5$ this introduces an uncertainty of only $\Delta_{\rm I} = \pm 0.003$ in $\log(M/L)$. (Here and henceforth we denote sources of systematic uncertainty in $\log(M/L)$ with a roman numeral subscript. A summary listing of all sources of systematic uncertainty encountered in this paper is presented in Table 1.) The uncertainties in H_0 and their effect on $\log(M/L)$ will be addressed later.

2. LOCAL GALAXY MASS-TO-LIGHT RATIO COMPARISON SAMPLE

2.1. *Dynamical Modeling Sources*

To study the M/L evolution with redshift we need a comparison sample of dynamically inferred M/L values for *nearby* early-type galaxies. We restrict our attention here to five detailed dynamical modeling studies that addressed relatively large samples: van der Marel (1991, hereafter vdM91); Magorrian et al. (1998, hereafter M98); Kronawitter et al. (2000, hereafter K00); Gebhardt et al. (2003, hereafter G03); and Cappellari et al. (2006a, hereafter C06). These studies differ from each other in many ways, both in terms of the quality and nature of the data that were used, and in the methods and sophistication of the modeling. In particular:

- vdM91 and K00 used ground-based photometry, whereas M98, G03 and C06 used a combination of both HST and ground-based photometry;
- vdM91, M98, K00 and C06 used ground-based spectroscopy, whereas G03 used a combination of ground-based and HST spectroscopy;
- vdM91, M98, K00 and G03 used long-slit spectroscopy along one or more slit position angles, whereas C06 used fully two-dimensional integral-field spectroscopy;
- K03 constructed spherical dynamical models (they restricted their sample to galaxies that are almost circular in projection on the sky), whereas vdM91, M98, G03 and C06 constructed axisymmetric models;
- vdM91 and M98 constructed two-integral models using the Jeans equations, K00 constructed models using an expansion around a set of known basis distribution functions, and G03 and C06 constructed fully general models using numerical orbit superposition;
- K00 included kinematical data in the central few arcsec in their fits, but did not allow for the possible gravitational contribution of a central BH; vdM91 also did not include a BH in the models but excluded the central few arcsec from the fit; C06 included a BH of fixed mass in the models but still excluded the central few arcsec from the fit; and M98 and G03 included BHs in their models and fitted their masses by using the data in the central few arcsec;
- vdM91, M98, G03 and C06 assumed a constant value of M/L with radius, whereas K03 explicitly included (and optimized) the contribution of a dark halo;
- K03 determined M/L values in the B-band, M98 and G03 in the V-band,[1] vdM91 in the Johnson $R_{\rm J}$ band, and C06 in the I-band.

We purposely included the results from all five studies, rather than to retain merely a smaller sample composed of the most recent or most accurate results. One advantage of this it that by comparing the results from the different studies we are able to put firm limits on various kinds of potential systematic uncertainties.

2.2. *Distances*

It is important for our study to use a set of galaxy distances that is as accurate and homogeneous as possible.

[1] G03 reported the M/L for one galaxy, NGC 4564, in the I-band.

For this we follow the example of G03 and C06 by using the compilation of Tonry et al. (2001, hereafter T01). They obtained distances to 300 nearby galaxies, mostly of early type, using the surface brightness fluctuation (SBF) method. We removed from our initial sample of 81 total galaxies in vdM91, M98, K00, G03 and C06 the 17 galaxies that are not part of the T01 sample. We rejected two more galaxies (M31 and NGC 4594) because they are not early-type galaxies (which we define here as Hubble type $T < 0$) and two other galaxies (NGC 3384 and NGC 7332) for the reasons discussed in Section 2.4. Table 2 lists the final sample of 60 galaxies and includes for each galaxy, among other things, the Hubble type T and the adopted distance modulus and its uncertainty. The average distance for the sample galaxies is 21.6 Mpc. This corresponds to $\langle z \rangle = 0.005$, given the Hubble constant listed in Section 1.

There are 6 spiral galaxies with bulges in common between the SBF sample of T01 and the sample of galaxies for which Cepheid distances are available from the HST Cepheid Key Project. T01 calibrated the zeropoint of their SBF method so as to set to zero the *median* SBF vs. Cepheid distance modulus residual for these 6 galaxies (see Appendix B of Tonry et al. 2000). This was done using Cepheid results available in 2000. These Cepheid distances have since been improved (Freedman et al. 2001). Application of the same calibration methodology to the new Cepheid distances implies an SBF zeropoint that is larger by +0.06 mag (e.g., Mei et al. 2005). To account for this, we added a correction $\Delta_{\rm T01} = -0.06$ mag to all the distance moduli in T01 (i.e., moving the galaxies closer).

For the purposes of our study it is important to understand the accuracy with which the SBF and Cepheid distance scales have been aligned. If one uses the weighted average rather than the median statistic to align the 6 spiral galaxies, then the SBF zeropoint changes by −0.12. Alternatively, if one chooses not to align the distance scales using individual galaxies at all, but instead using distances to groups of galaxies (Ferrarese et al. 2000), then this yields a change of −0.13 to the SBF zeropoint (Tonry et al. 2000). And finally, if one changes the SBF zeropoint by +0.10, then better agreement is obtained with predictions of population synthesis models (Jensen et al. 2003).[2] Based on these considerations we assume that the systematic uncertainty on $\Delta_{\rm T01}$ is ±0.13 mag. This corresponds to an uncertainty $\Delta_{\rm II} = \pm 0.026$ in $\log(M/L)$.

After its calibration to agree with Cepheids, the SBF distance scale is subject to all the same absolute distance scale uncertainties that are inherent to the Cepheid distance scale. These are summarized in Section 8 and Table 14 of Freedman et al. (2001). Most of the uncertainties affect both the distances of local galaxies, as well as the inferred value of H_0. They include: the distance to the LMC, the photometric zeropoint of the HST/WFPC2 used for the Cepheid studies, the accuracy of the reddening and metallicity corrections applied to the Cepheids, and biases introduced by crowding and the magnitude limit of the sample. When added in quadrature, as in Freedman et al. (2001), these effects introduce a 9% systematic uncertainty in the galaxy distances. This corresponds to a difference $\Delta_{\rm III} = \pm 0.037$ in $\log(M/L)$. This uncertainty must be taken into account, e.g., when comparing the M/L values of local galaxies to the predictions of stellar population synthesis models.

The systematic Cepheid distance scale uncertainties listed in the previous paragraph do *not* affect a relative comparison of M/L values of nearby and distant galaxies. Any shift in the overall distance scale of the Universe would affect both types of galaxies equally, and would therefore cancel out when evaluating a difference in $\log(M/L)$. The only distance scale uncertainties that do affect such a comparison are those that impact the estimate of H_0, but not the Cepheid distances to local galaxies. These uncertainties have both a systematic and a random component. The systematic component is due to cosmic variance, i.e., the effect that local samples of galaxies may yield an estimate of H_0 that differs from the true cosmic value as a result of bulk flows. Based on the discussion in Section 8.6 of Freedman et al. (2001) we estimate this systematic component to be less than 2% on the scales $z \lesssim 0.1$ over which Type Ia supernovae have been used to calibrate H_0. This corresponds to a difference $\Delta_{\rm IV} = \pm 0.009$ in $\log(M/L)$. Random uncertainties in H_0, as opposed to systematic ones, result from finite sample sizes and scatter between results from individual measurements. Based on Section 7 of Freedman et al. (2001) we estimate the random uncertainty to be $\Delta H_0 = \pm 4\ {\rm km\,s^{-1}\,Mpc^{-1}}$. This corresponds to $\Delta_{\rm V} = \pm 0.023$ in $\log(M/L)$.

2.3. *Transformations to the B-band*

For comparison to results at intermediate redshifts it is important to have access to M/L values in the rest-frame B-band. We therefore took the published values[3] and transformed them to B-band mass-to-light ratios M/L_B for the distances D discussed in Section 2.2 using

$$M/L_B = (M/L_F)\,(D_{\rm orig}/D)\,10^{0.4[(B-F)-(B-F)_\odot]}. \quad (1)$$

Here M/L_F is the mass-to-light ratio in some other band F for the distance $D_{\rm orig}$, as given in the original literature source; $B-F$ is the relevant broad-band color of the galaxy, and $(B-F)_\odot$ is the color of the sun.

For the transformation in equation (1) we needed colors of the sample galaxies in various bands. For $B-V$ we used the data of Faber et al. (1989, hereafter F89), who presented data for almost 600 nearby early-type galaxies. Their colors refer to apertures $\leq 30''$ in diameter around the galaxy center. The average color for the galaxies in our sample is $\langle B-V \rangle = 0.95$. We used this average color for the 8 galaxies in our final sample for which a $B-V$ was needed but for which none was available from

[2] This zeropoint also happens to align the SBF distance scale with the Cepheid distance scale *if* one assumes that the Cepheid properties have no metallicity dependence. But that is not what Freedman et al. (2001) assumed in their final calibration. Comparisons of TRGB and Cepheid distances also indicate a Cepheid metallicity dependence (Sakai et al. 2004). The shift advocated by Jensen et al. (2003) was used by C06 in their study of M/L values of nearby galaxies.

[3] Some studies list multiple values of the M/L obtained under slightly different assumptions. For vdM91 we take the values labeled $\Upsilon_R^{\rm imp}$ in his Table 2. For K00 we take the central value labeled "best $M/L_B^{\rm c}$" in their Table 7. For C06 we take the values from their Schwarzschild models, labeled $(M/L)_{\rm Schw}$ in their Table 1, as opposed to the values from their two-integral models.

TABLE 2
Local Galaxy Sample

Galaxy (1)	Type (2)	$m - M$ (3)	$\log \sigma_{\rm eff}$ (4)	$\log M/L_B$ (5)	vdM91 (6)	M98 (7)	K00 (8)	G03 (9)	C06 (10)
NGC 0221	-6	24.49 ± 0.08	-0.481	0.403 ± 0.053		X			X
NGC 0524	-1	31.84 ± 0.20	0.064	1.022 ± 0.067					X
NGC 0636	-5	32.31 ± 0.16	-0.134	0.694 ± 0.116	X				
NGC 0720	-5	32.15 ± 0.17	0.049	1.034 ± 0.116	X				
NGC 0821	-5	31.85 ± 0.17	-0.022	0.881 ± 0.049		X		X	X
NGC 1052	-5	31.38 ± 0.27	-0.020	1.026 ± 0.116	X				
NGC 1379	-5	31.45 ± 0.15	-0.212	0.582 ± 0.116	X				
NGC 1395	-5	31.85 ± 0.16	0.069	0.921 ± 0.116	X				
NGC 1399	-5	31.44 ± 0.16	0.155	1.024 ± 0.059	X	X	X		
NGC 1404	-5	31.55 ± 0.19	0.026	0.896 ± 0.116	X				
NGC 1407	-5	32.24 ± 0.26	0.097	1.057 ± 0.116	X				
NGC 1439	-5	32.07 ± 0.15	-0.149	0.777 ± 0.116	X				
NGC 1549	-5	31.41 ± 0.18	-0.027	0.763 ± 0.116	X				
NGC 1700	-5	33.17 ± 0.16	0.039	0.842 ± 0.116	X				
NGC 2434	-5	31.61 ± 0.29	-0.026	0.938 ± 0.117			X		
NGC 2778	-5	31.74 ± 0.30	-0.097	0.975 ± 0.071		X		X	
NGC 2974	-5	31.60 ± 0.24	0.074	0.989 ± 0.067					X
NGC 3115	-3	29.87 ± 0.09	0.109	0.995 ± 0.085		X			
NGC 3156	-2	31.69 ± 0.14	-0.420	0.349 ± 0.067					X
NGC 3193	-5	32.60 ± 0.18	-0.025	0.711 ± 0.117			X		
NGC 3377	-5	30.19 ± 0.09	-0.194	0.571 ± 0.049		X		X	X
NGC 3379	-5	30.06 ± 0.11	-0.009	0.821 ± 0.044	X	X	X		X
NGC 3414	-2	31.95 ± 0.33	0.002	0.925 ± 0.067					X
NGC 3557	-5	33.24 ± 0.22	0.112	0.842 ± 0.116	X				
NGC 3608	-5	31.74 ± 0.14	-0.058	0.851 ± 0.045	X	X		X	X
NGC 3640	-5	32.10 ± 0.13	-0.092	0.694 ± 0.117			X		
NGC 4150	-2	30.63 ± 0.24	-0.438	0.378 ± 0.067					X
NGC 4168	-5	32.39 ± 0.42	-0.089	0.929 ± 0.069		X	X		
NGC 4261	-5	32.44 ± 0.19	0.123	1.146 ± 0.116	X				
NGC 4278	-5	30.97 ± 0.20	0.064	0.996 ± 0.048		X	X		X
NGC 4291	-5	32.03 ± 0.32	0.095	0.943 ± 0.071		X		X	
NGC 4374	-5	31.26 ± 0.11	0.151	0.992 ± 0.052	X		X		X
NGC 4406	-5	31.11 ± 0.14	0.047	0.904 ± 0.116	X				
NGC 4458	-5	31.12 ± 0.12	-0.403	0.638 ± 0.067					X
NGC 4459	-1	30.98 ± 0.22	-0.089	0.710 ± 0.067					X
NGC 4472	-5	31.00 ± 0.10	0.105	1.029 ± 0.059	X	X	X		
NGC 4473	-5	30.92 ± 0.13	-0.018	0.816 ± 0.049		X		X	X
NGC 4486	-4	30.97 ± 0.16	0.208	1.139 ± 0.044	X	X	X		X
NGC 4494	-5	31.10 ± 0.11	-0.239	0.719 ± 0.082	X		X		
NGC 4526	-2	31.08 ± 0.20	0.051	0.836 ± 0.067					X
NGC 4550	-2	30.94 ± 0.20	-0.252	0.685 ± 0.067					X
NGC 4552	-5	30.87 ± 0.14	0.099	0.986 ± 0.053		X			X
NGC 4564	-5	30.82 ± 0.17	-0.129	0.792 ± 0.071		X		X	
NGC 4589	-5	31.65 ± 0.22	-0.006	1.071 ± 0.117			X		
NGC 4621	-5	31.25 ± 0.20	0.025	0.846 ± 0.053		X			X
NGC 4636	-5	30.77 ± 0.13	-0.069	1.089 ± 0.059	X	X	X		
NGC 4649	-5	31.07 ± 0.15	0.188	1.053 ± 0.060	X	X		X	
NGC 4660	-5	30.48 ± 0.19	-0.034	0.873 ± 0.053		X			X
NGC 4697	-5	30.29 ± 0.14	-0.120	0.918 ± 0.086	X			X	
NGC 5813	-5	32.48 ± 0.18	0.061	0.990 ± 0.067					X
NGC 5845	-5	32.01 ± 0.21	0.077	0.872 ± 0.060				X	X
NGC 5846	-5	31.92 ± 0.20	0.104	1.115 ± 0.052	X		X		X
NGC 6703	-3	32.07 ± 0.29	-0.097	0.749 ± 0.117			X		
NGC 7144	-5	31.89 ± 0.12	-0.074	0.840 ± 0.116	X				
NGC 7145	-5	31.79 ± 0.21	-0.218	0.761 ± 0.082	X		X		
NGC 7192	-4	32.83 ± 0.32	-0.080	0.665 ± 0.117			X		
IC 1459	-5	32.27 ± 0.28	0.145	0.912 ± 0.116	X				
NGC 7457	-3	30.55 ± 0.21	-0.444	0.550 ± 0.060				X	X
NGC 7507	-5	31.93 ± 0.17	0.042	0.801 ± 0.082	X		X		
NGC 7619	-5	33.56 ± 0.31	0.175	1.002 ± 0.116	X				

Note. — Column (1) lists the galaxy name. Columns (2) and (3) list the morphological type and distance modulus from T01; the T01 values were shifted by -0.06 mag to align the SBF distance scale with the Cepheid distance scale. Column (4) lists the base-10 logarithm of $\sigma_{\rm eff}$ in km/s, either taken directly from C06 or otherwise calculated from the data in F89. We assume the uncertainties on $\log(\sigma_{\rm eff})$ to be 0.021. Column (5) lists the base-10 logarithm of (M/L_B) and its uncertainty, obtained through weighted combination of the results from different studies. (The uncertainties should not be used for studies of the intrinsic scatter in relations between M/L and other global galaxy properties, because they were derived under the assumption that the intrinsic scatter in the correlation with $\sigma_{\rm eff}$ is negligible.) Columns (6)–(10) indicate the original dynamical modeling sources from which the M/L values were obtained: van der Marel (1991, vdM91); Magorrian et al. (1998, M98); Kronawitter et al. (2000, K00); Gebhardt et al. (2003, G03); or Cappellari et al. (2006a, C06).

F89. For those galaxies for which we needed the color $B-R_{\rm J}$ we used the transformation $B-R_{\rm J}=1.839(B-V)+0.064$. This was obtained from the equations $B-R_{\rm J}=1.14(B-R_{\rm C})+0.04$ and $V-R_{\rm C}=0.613(B-V)+0.021$ derived for early-type galaxies by Peletier et al. (1990). The subscripts in these equations refer to the Johnson and the Cousins R-band, respectively. The implied average color of the sample is $\langle B-R_{\rm J}\rangle=1.81$.

For the transformation of M/L values in the I-band we needed the $B-I$ colors of the galaxies. We calculated those as the sum of $B-V$ and $V-I$, with the former from F89 and the latter from T01. However, a small correction was needed to the T01 colors because they apply to an annular region around the galaxy center. The dynamical M/L determinations are therefore more heavily weighted towards the galaxy center than the T01 colors. The central region that was excluded by T01 has an average diameter of $24''$ for those galaxies in our sample for which the original M/L was given in the I-band. The average color of these galaxies is $\langle(V-I)_{\rm T01}\rangle=1.16$. Early-type galaxies become redder towards their centers, and this implies that the T01 colors are bluer than the ones that should be used in equation (1). As a simple correction for this we used $V-I=(V-I)_{\rm T01}+\epsilon$. We applied this equation on a galaxy-by-galaxy basis, but the small constant ϵ was chosen to be a fixed number. To set its value we compared to the predictions of stellar population synthesis models. The central colors $\langle B-V\rangle=0.95$ and $\langle B-R_{\rm J}\rangle=1.81$ of early-type galaxies in our sample are fit to within 0.01 mag by a $10^{9.97}$ yr old single age stellar population with a Chabrier IMF of solar metallicity and solar abundances ratios (Bruzual & Charlot 2003).[4] Such a population has $V-I=1.20$ (Bruzual & Charlot 2003). To make the average T01 colors consistent with these stellar population predictions we therefore choose $\epsilon=0.04$. The sign and size of this offset is consistent with our understanding of the $V-I$ color gradients in the centers of early-type galaxies (Lauer et al. 2005).

In equation (1) we also needed the colors of the sun. Throughout this paper we use the solar absolute magnitudes compiled by Binney & Merrifield (1998): $M_\odot=5.48(B),4.83(V),4.42(R_{\rm C})$, and $4.08(I)$. For the transformation of the vdM91 results we needed also the solar absolute magnitude in the Johnson R-band. For this we used the color transformation $R_{\rm J}=R_{\rm C}-0.12(B-R_{\rm C})-0.07$ (Davis et al. 1985) to obtain $M_\odot=4.22(R_{\rm J})$.[5]

2.4. *Velocity Dispersions*

For the analysis and interpretation of the results it is important to have access also to other characteristic quantities for the sample galaxies. The velocity dispersion is particularly useful, because it has been found to correlate strongly with the galaxy M/L (C06). To characterize the dispersion we chose the value $\sigma_{\rm eff}$ inside an aperture of size equal to the effective radius $r_{\rm eff}$. C06 directly measured this quantity for the galaxies in their sample from their own data, and we adopted their values for those galaxies. For the remainder of the galaxies in our sample we started from the values $\sigma_{\rm nuc}$ given by F89. These are averages of observed values from different observational setups, corrected to the size of a few-arcsec aperture at the distance of Coma. From these values we estimated the dispersion in an aperture of size $r_{\rm eff}$, using the values of $r_{\rm eff}$ also given by F89 and the correction formulae given in Jorgensen et al. (1995b). The two galaxies NGC 3384 and NGC 7332 did not have data available from either C06 or F89, and we removed these galaxies from the sample.

The uncertainties in $\sigma_{\rm eff}$ are probably not dominated by random uncertainties due to the finite S/N of the spectroscopy, but by systematic uncertainties associated with template mismatch, continuum subtraction, and other issues. For the high-quality integral field data of C06 we followed those authors and estimated the uncertainties in $\sigma_{\rm eff}$, somewhat conservatively, to be $\sim5\%$ (see also Tremaine et al. 2002). This implies $\Delta\log\sigma_{\rm eff}=0.021$. For those galaxies for which a dispersion estimate is available also from the F89 data we find that the residuals $\delta\log\sigma_{\rm eff}\equiv\log\sigma_{\rm eff,F89}-\log\sigma_{\rm eff,C06}$ are on average consistent with zero: $\langle\delta\log\sigma_{\rm eff}\rangle=-0.007\pm0.008$. The RMS scatter in the residuals is 0.031.[6] This is approximately what would be expected if the $\sigma_{\rm eff}$ values inferred from the F89 data also have uncertainties of $\sim5\%$, which is therefore what we assumed.

Table 2 lists the inferred $\sigma_{\rm eff}$ for all galaxies. The table does not list other galaxy parameters that we will not use here. However, we note that various other quantities can be obtained relatively easily. Effective radii are available from C06 or F89. The latter authors also provide $I_{\rm eff}$, the average B-band surface brightness inside the effective radius. The total B-band luminosity can be estimated from $L=2\pi r_{\rm eff}^2 I_{\rm eff}$, or it can be obtained from the apparent B-band magnitudes listed in, e.g., the RC3 (de Vaucouleurs et al. 1991). A characteristic mass[7] can be obtained upon multiplication by the M/L listed in the table.

2.5. *Mass-to-Light Ratio Accuracies and Correlations*

The random uncertainties on the M/L estimates can be divided broadly in two components: distance uncertainties and dynamical uncertainties. The random distance uncertainties come from the finite accuracy of the SBF measurements. They contribute in quadrature $\Delta\log(M/L)=0.2\Delta(m-M)$, where $\Delta(m-M)$ is the uncertainty in the distance modulus from T01. The dynamical uncertainties can come from a large variety of sources, e.g., shortcomings in the kinematical data or their spatial coverage, or limitations in the modeling or its underlying assumptions. As a result, they are generally poorly quantified. We quantify the random dynamical uncertainties through a parameter E which for

[4] This does not necessarily mean that the stellar populations are indeed on average $10^{9.97}$ yr old, and have solar metallicity and solar abundances ratios. But it does mean that such models predict the correct continuum slope when compared to observations of the centers of nearby early-type galaxies. The models can therefore be used to estimate the broad-band colors in filter combinations for which observations are not directly available.

[5] vdM91 had used $M_\odot=4.31(R_{\rm J})$, so we corrected his results to $M_\odot=4.22(R_{\rm J})$ before application of equation (1).

[6] This scatter was obtained by comparing only galaxies with $\sigma_{\rm eff}>100\,{\rm km\,s^{-1}}$, as appropriate for all the galaxies in our sample for which we actually use the F89 data. We did find larger residuals of ~0.1 dex for the few galaxies with $\sigma_{\rm eff}<100\,{\rm km\,s^{-1}}$.

[7] The mass $M\equiv(M/L)\times L$ is smaller than the total galaxy mass, because it doesn't include all the contribution from a dark halo. However, it may contain some contribution from dark matter (K00, C06), so it is probably larger than the total mass in stars.

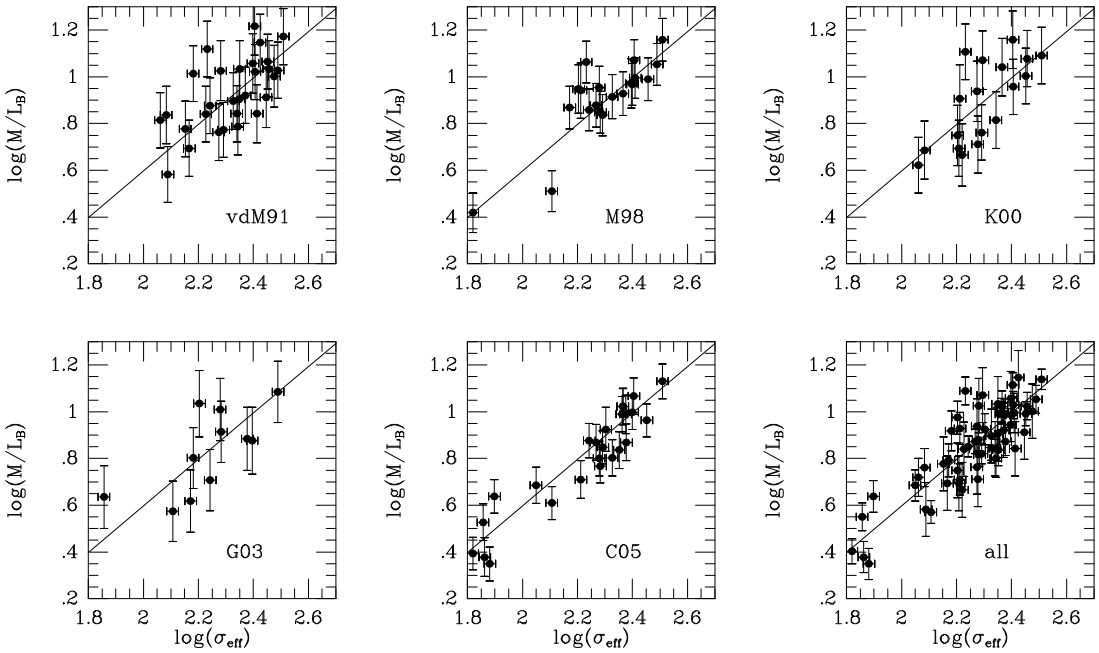

FIG. 1.— Correlation of M/L (in solar units) with $\sigma_{\rm eff}$ (in km/s) for nearby early-type galaxies. The M/L measurements from the dynamical studies of van der Marel (1991, vdM91), Magorrian et al. (1998, M98), Kronawitter et al. (2000, K00), Gebhardt et al. (2003, G03) and Cappellari et al. (2006a, C06) are shown in separate panels. All measurements were transformed to the B band and to a homogeneous set of SBF distances. The bottom-right panel contains the combined dataset from Table 2. The solid line (the same in each panel) is the best fit to this combined data set.

simplicity we assume to be a constant for all the measurements in a given dynamical study. We then set the total random uncertainty $\Delta\log(M/L)$ for a measurement in a given study equal to the sum of the random distance uncertainty for the galaxy in question and the value of E for that study.

To estimate the random uncertainty E for each study we use the fact that the M/L correlates with other global galaxy properties. Previous work has shown that there are good correlations with either luminosity or mass (vdM91, M98), as expected to explain the "tilt" of the FP. More recently, C06 showed that the M/L correlates even better, i.e., with lower scatter, with $\sigma_{\rm eff}$. This is the correlation that we will use here. For each individual dynamical study we selected the M/L_B values for the galaxies in our final sample and then fitted a straight line of the form

$$\log(M/L_B) = Z + S\log(\sigma_{\rm eff}/[200\,{\rm km\,s^{-1}}]); \qquad (2)$$

here "Z" is short for zeropoint, and "S" is short for slope. We will refer to this as the M/L–σ relation. The fit was performed with the routine fitexy of Press et al. (1992), which takes into account the uncertainties in both independent variables. The value of E for each study was then chosen so as to yield a χ^2 of the fit that is equal to the number of degrees of freedom. This assumes implicitly that there is no intrinsic scatter in the correlation, which is conservative in the sense that it yields the largest possible random uncertainties. Application of this procedure yields $E = 0.116$ dex for vdM91, $E = 0.085$ dex for M98, $E = 0.117$ dex for K00, $E = 0.128$ for G03, and $E = 0.067$ dex for C06. Figure 1 shows the final B-band M/L values and their random uncertainties as a function of $\sigma_{\rm eff}$ for all five of the individual dynamical studies.

To obtain a combined M/L_B estimate and uncertainty for each individual galaxy we used a two-step procedure. First we took the weighted average of the M/L_B values inferred from the different studies of that galaxy, using the uncertainties E listed above to set the weights. Then we increased the uncertainty in the weighted average by adding in quadrature the random uncertainty $\Delta\log(M/L) = 0.2\Delta(m-M)$ introduced by distance uncertainties. Table 2 lists the final M/L_B estimates thus obtained for all galaxies.

The bottom right panel of Figure 1 shows the best straight line fit to the final combined data set. It has parameters $Z = 0.896 \pm 0.010$ and $S = 0.992 \pm 0.054$. This same line is shown as a solid line in all panels of Figure 1. The slope of the relation differs significantly from the best-fit slope S_I[C06] $= 0.82 \pm 0.06$ found by C06 for the I-band. This is not due to the use of a different galaxy sample. If we perform a linear fit to only the M/L_B values derived from the C06 study we infer S[C06] $= 0.991 \pm 0.076$, consistent with the value of S inferred for the full sample. The difference in slope between the I- and B-bands is therefore real, and is due to the well-known fact that galaxies of low dispersion (or mass) tend to bluer than those of high dispersion.

Figure 1 shows that the different studies are all entirely consistent with each other. When the data from each study are fitted individually with a straight line, the best fit slope is always consistent with the value $S = 0.992 \pm 0.054$ inferred for the full sample to within 1.2σ or better. When the data from each study are fitted individually with a straight line of fixed slope $S = 0.992$, the inferred zeropoints are: Z[vdM91] $= 0.914 \pm 0.023$, Z[M98] $= 0.912 \pm 0.021$, Z[K00] $= 0.897 \pm 0.029$, Z[G03] $= 0.894 \pm 0.040$, and Z[C06] $= 0.876 \pm 0.017$. These zeropoints are all consistent with the value $Z = 0.896 \pm 0.010$ inferred for the full sample to within 1.2σ or better. The results from the C06 study have the smallest scatter in Figure 1, as quantified already by the param-

eter E. Judged also from the sophistication and homogeneity of their analysis, their results are probably the most reliable of the five studies that we have included in our sample. On the other hand, the color transformations that we had to apply to transform their I-band results to the B-band are probably more uncertain than the transformations that we had to apply to some of the other studies. This may be the root cause of the fact that the zeropoint for the C06 data is offset from that for the full sample by -0.020. Either way, the more important conclusion in this context is that the zeropoint of the relation is quite robust.[8] The use of vastly different data and models among 5 different studies does not alter the zeropoint of the relation by more than $\Delta_{\rm VI} = \pm 0.020$. We adopt this as the systematic uncertainty in our knowledge of the zeropoint Z from dynamical modeling limitations. The robustness of M/L estimates from different modeling approaches is consistent with several findings reported by C06. For example, they find that the results of axisymmetric modeling generally do not depend strongly on the assumed inclination. They also find that even though two-integral and three-integral models yield subtly different M/L estimates, there is little bias in the inferred average M/L for a sample that has a typical range of M/L values.[9]

We are now in a position to combine all the various sources of systematic uncertainty that enter into the zeropoint Z_B of equation (2). These are the uncertainties labeled II, III, and VI in Table 1. We assume that systematic uncertainties can be added in quadrature. The final estimate of the B-band zeropoint for local galaxies is then

$$Z_{0.005} = 0.896 \pm 0.010({\rm random}) \pm 0.049({\rm systematic}), \quad (3)$$

where the value $\langle z \rangle = 0.005$ listed in the subscript is the average redshift of the sample galaxies.

3. MASS-TO-LIGHT RATIO EVOLUTION

3.1. *Intermediate-Redshift Cluster Galaxy Sample*

The sample of Paper I consists of 25 galaxies that reside in the clusters CL 3C295, CL 0016+1609, and CL 1601+4253, at redshifts $z = 0.456$, 0.546, and 0.539, respectively (Dressler & Gunn 1992; Dressler et al. 1999). The clusters were selected based on their visibility at the time of the Keck observations, and because they are among the most S0 deficient clusters in the MORPHS sample (Dressler et al. 1997). The latter criterion has little relevance for the results discussed in the present paper, but was relevant for the discussion of the rotation properties of the sample galaxies presented in Paper I. The MORPHS sample itself was not selected according to strict criteria. The galaxy selection was largely constrained by the geometry of the Keck/LRIS masks, and by the fact that sample galaxies should be bright enough for spectroscopy. Priority was given to galaxies classified from HST images as E or E/S0 by Smail et al. (1999). The latest-type galaxy included in the sample was an S0/Sb galaxy. This galaxy 3C295-568 was included for the specific purpose to see if rotation could reliably measured (which is indeed the case, as demonstrated in Paper I).

The galaxy CL 3C295-2014 is the well-known AGN 3C295. There is the possibility that this galaxy contains a central non-thermal point source that could bias the analysis. However, the results for both the light profile of this galaxy and its M/L (see Paper I and the discussion in Section 3.2 below) do not provide any evidence for deviations from the trends defined by the other galaxies in the sample. We therefore retained CL 3C295-2014 in our sample and did not treat it in any special way.

3.2. *Evolution of the M/L–σ relation*

Figure 2b shows the M/L–σ relation for our sample of intermediate-redshift cluster galaxies, using the data from Table 1 in Paper I. We estimate the systematic uncertainties in velocity dispersion estimates to be $\sim 5\%$, as in Section 2.4 (i.e., $\Delta \log \sigma_{\rm eff} = 0.021$). These uncertainties were added in quadrature to the random uncertainties from Paper I before plotting and analysis. For comparison, the left panel of Figure 2a shows the M/L–σ relation for local galaxies, as in the bottom right panel of Figure 1.

The solid line in Figure 2b is the line with the fixed slope $S = 0.992$ (as inferred from the local galaxy sample) that best fits the intermediate redshift cluster galaxies. It has zeropoint

$$Z_{0.528} = 0.657 \pm 0.022({\rm random}) \pm 0.049({\rm systematic}). \quad (4)$$

The value $\langle z \rangle = 0.528$ listed in the subscript is the average redshift of the galaxies. The random uncertainty in the zeropoint was determined as the ratio of the RMS residual with respect to the fit and $\sqrt{N}$, where $N = 24$ is the number of galaxies. This does not include the S0/Sb galaxy CL 3C295-568, which was excluded from the analysis because it is not an early-type galaxy (defined here as $T < 0$). By estimating the random zeropoint uncertainty in this way we do not use the random uncertainties $\Delta \log(M/L)$ in the individual M/L measurements listed in Paper I. The average of these uncertainties is actually smaller than the scatter around the best fit (0.051 vs. 0.108, respectively). This may be due to the presence of additional random uncertainties in addition to those propagated from the observed kinematics, or it may be due to intrinsic scatter in the M/L–σ relation. The systematic uncertainty listed in equation (4) is the quadrature sum of the relevant uncertainties, namely I, III, IV, V and VI in Table 1. This assumes, in analogy with the local sample, that the systematic uncertainty due to modeling limitations is $\Delta_{\rm VI} = \pm 0.020$. This is reasonable, because the two-integral modeling that we have used for the intermediate-redshift cluster sample was very similar to that used by vdM91 and M98 for local galaxies (and more generally, C06 found that two-integral models do not yield strongly biased M/L estimates as compared to more sophisticated three-integral models).

The evolution of the M/L between the two redshifts is obtained by subtracting the zeropoints of the M/L–σ relations given by equations (3) and (4). This yields

$$\delta \log(M/L) \equiv Z_{\rm distant} - Z_{\rm local} = -0.239 \pm 0.024\,({\rm random}) \pm 0.041\,({\rm systematic}), \quad (5)$$

[8] An alternative way to assess differences in zeropoint between different studies is to analyze the M/L values for those galaxies that have measurements from more than one study. We have performed such an analysis and found zeropoint differences that are consistent with those obtained from the M/L–σ relation.

[9] The averages of all the log M/L estimates in the C06 sample for two- and three-integral models respectively agree to within 0.003.

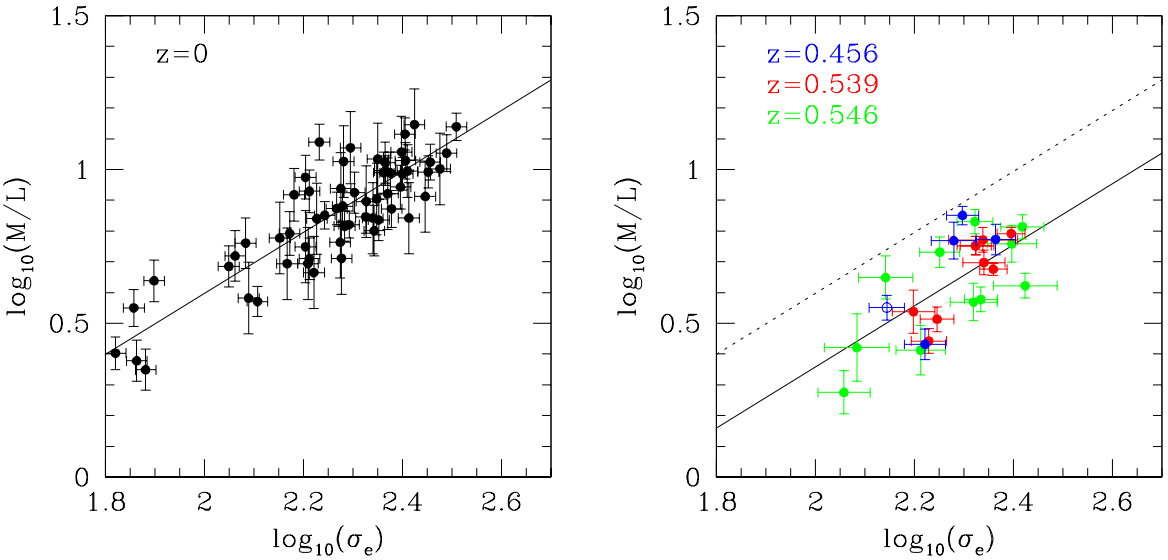

FIG. 2.— (a) M/L–σ relation for the sample of local galaxies listed in Table 2 (same as in the bottom right panel of Figure 1). The solid line is the best linear fit. (b) The same quantities, but now for the sample of intermediate redshift cluster galaxies modeled in Paper I. The galaxies are color-coded by the cluster in which they reside: CL 3C295 (blue), CL 1601+4253 (red) or CL 0016+1609 (green). The cluster redshifts are labeled on the plot. The dotted line is the best-fit for local galaxies (as also shown in the left panel). The solid line has the same slope, but was shifted to best fit the intermediate redshift cluster galaxies. This shift quantifies the M/L evolution with redshift. The open symbol denotes the S0/Sb galaxy CL 3C295-568, which was excluded from the analysis of M/L evolution because it is not an early-type galaxy (defined here as $T < 0$).

where in this particular case the average redshifts for the distant and local samples are $\langle z \rangle = 0.528$ and 0.005, respectively. The random uncertainty in $\delta \log(M/L)$ is simply the quadrature sum of the random uncertainties in $Z_{0.528}$ and $Z_{0.005}$. However, the systematic uncertainty is not the quadrature sum of the systematic uncertainties in those quantities. That is because source III of systematic uncertainty in Table 1 is common to both zeropoints, and therefore drops out of their difference. So the systematic uncertainty listed in equation (5) is the quadrature sum of the uncertainties I, II, IV, V and VI in Table 1. We include source VI only once, because it was defined as a measure of the typical difference in the results from different dynamical modeling approaches.

As discussed in Paper I, the only parameter in our models that is not generally constrained by the data is the inclination, or alternatively, the intrinsic axial ratio Q. Equation (5) was derived from the results obtained in Paper I for our "standard inclination" models. These models use for each galaxy the most likely inclination, given the observed projected axial ratio. These models have the correct average intrinsic axial ratio when averaged over a large sample. For comparison we have also constructed two sets of alternative models, namely models that are edge-on (yielding the roundest possible intrinsic shape for each galaxy) and models that have intrinsic axial $Q_{\rm min} = 0.4$ (which is approximately the smallest intrinsic axial ratio found for early-type galaxies). The former yield an average $\delta \log(M/L)$ for the sample that is lower by -0.008 than for the standard inclination models. The latter yield a value that is higher by 0.053. The assumptions that underly these models are clearly unrealistic for the sample as a whole, and either way do not change the result in equation (5) by much more than the listed uncertainties. Nonetheless, these numbers give some idea of the systematic uncertainty in the M/L estimates *for individual galaxies* due to the unknown inclinations. In other words, variations in inclination between galaxies of the same projected axial ratio do not affect the average correlation in Figure 2b, but they do add to the scatter. However, the induced scatter is too small to account for the observed scatter of 0.108 in $\log(M/L)$.

The change of M/L with redshift is $\Delta \log(M/L)/\Delta z = \delta \log(M/L)/(\langle z \rangle_{\rm distant} - \langle z \rangle_{\rm local})$. Equation (5) thus gives

$$\Delta \log(M/L)/\Delta z = -0.457 \pm 0.046\,({\rm random}) \pm 0.078\,({\rm systematic}) \quad (6)$$

So far we have treated all intermediate redshift cluster galaxies as a single sample. It is of course also possible to calculate the zeropoint evolution for each cluster individually. This yields $\delta \log(M/L)$ (CL 3C295) $= -0.180 \pm 0.065$ (random), $\Delta \log(M/L)$ (CL 1601+4253) $= -0.259 \pm 0.035$ (random), and $\Delta \log(M/L)$ (CL 0016+1609) $= -0.241 \pm 0.024$ (random). These values each have the same systematic uncertainty as listed for the combined sample in equation (5). The cluster CL 3C295 has the smallest amount of evolution, as expected given its lower redshift. However, the differences between the clusters are not really significant given the random uncertainties. The clusters span a range $\Delta z = \pm 0.045$ (see Section 3.1), which implies an expected variation $\Delta \log(M/L) = \pm 0.02$ on the basis of equation (6). This is smaller than the average random error of 0.051 in our $\log(M/L)$ measurements, and it is also smaller than the scatter of 0.108 around the linear fit in Figure 2b. Correction for differential evolution between galaxies in our sample at slightly different redshifts would therefore not change any of the results. So it is justified to treat the galaxies as a single sample at an average redshift $\langle z \rangle = 0.528$. This approach has the advantage that it doesn't introduce any prior knowledge about evolution into the analysis of the sample.

TABLE 3
Sources of systematic uncertainty that affect Fundamental Plane zeropoints

ID	$\Delta\zeta$	source of systematic uncertainty	Section
I	±0.003	effect of uncertainties in $\Omega_{\rm m}$ and Ω_Λ at $z \approx 0.5$	1
III	±0.037	accuracy of the Cepheid distance scale for local galaxies	2.2
IV	±0.009	cosmic variance in H_0 on the scale $z \lesssim 0.1$	2.2
V	±0.023	random uncertainty in H_0 due to finite sample sizes	2.2
VII	±0.013	uncertainty in Hubble flow velocity of Coma	3.3
VIII	±0.020	difference in FP zeropoint determinations from different authors, at fixed distance	3.3
IX	±0.018	cosmic variance in H_0 on the scale $z \lesssim 0.025$	3.3

Note. — Column (1) lists the roman numeral with which a particular systematic uncertainty is referred to in the text. Column (2) lists the size of the systematic uncertainty in the Fundamental Plane zeropoint ζ. The corresponding uncertainty in mass-to-light ratio is $\Delta\log(M/L) = \Delta\zeta/0.83$. Column (3) lists the source of the systematic uncertainty. Column (4) lists the number of the section in which the uncertainty is discussed.

3.3. *Comparison to Fundamental Plane evolution*

In vDvdM06 we studied the evolution of the FP of the sample clusters. The analysis used the relation

$$\log r_{\rm eff} = {\rm FP} - \zeta, \qquad (7)$$

where

$${\rm FP} \equiv 1.20\log\sigma_{\rm ap} - 0.83\log I_{\rm eff}. \qquad (8)$$

Here $\sigma_{\rm ap}$ is the dispersion in an aperture radius that spans $1.7''$ at the distance of the Coma cluster (this follows Jorgensen et al. 1995b) and $I_{\rm eff}$ is the average rest-frame B-band surface brightness inside $r_{\rm eff}$. From the shift in the zeropoint ζ of the relation with respect to the Coma cluster one infers an M/L evolution of

$$\begin{aligned}\delta\log(M/L) &\equiv (\zeta_{\rm distant} - \zeta_{\rm coma})/0.83 \\ &= -0.268 \pm 0.025\,({\rm random}) \pm 0.036\,({\rm systematic}). \end{aligned} \qquad (9)$$

This result uses only the same subset of $N = 17$ galaxies that were included in the FP analysis in vDvdM06 (we discuss this selection further in Section 4 below). It treats all the intermediate-redshift cluster galaxies as a single sample, for consistency with Section 3.2. The average redshift of this sample is $\langle z\rangle = 0.531$. The random uncertainty in $\delta\log(M/L)$ is $1/0.83$ times the quadrature sum of the random uncertainties in the FP zeropoints for Coma (0.011) and the intermediate-redshift cluster galaxy sample (0.023). For Coma we used the data for galaxies that have B-band photometry listed in Jorgensen et al. (1995a) and velocity dispersions listed in Jorgensen et al. (1995b). For each sample the random uncertainty was estimated as before as the ratio of the RMS residual with respect to the fit and $\sqrt{N}$.

The systematic uncertainty in equation (9) is due to a combination of the systematic uncertainties that affect $\zeta_{\rm coma}$ and $\zeta_{\rm distant}$. We summarize these uncertainties in Table 3. Sources that were already encountered previously are listed with the same roman numeral as in Table 1. Consider first the Coma FP zeropoint $\zeta_{\rm coma}$. Distance uncertainties affect $\log r_{\rm eff}$, and therefore the zeropoint of the FP relation. Distances in turn are estimated as the ratio of the Hubble flow velocity $v_{\rm flow}$ and the Hubble constant H_0. Uncertainties in both of these introduce FP zeropoint uncertainties. We have used in our analysis one of the most recent flow velocity estimates for Coma, namely $v_{\rm flow} = 7376 \pm 223\,{\rm km\,s^{-1}}$ from the SMAC survey (Smith, Lucey & Hudson 2006). This is consistent with several earlier results. For example, F89 obtained $v_{\rm flow} = 7461 \pm 273\,{\rm km\,s^{-1}}$ and Colless et al. (2001) obtained $v_{\rm flow} = 7238 \pm 302\,{\rm km\,s^{-1}}$. The uncertainties in all these results are dominated by the modeling uncertainty in the peculiar velocity $v_{\rm pec} \equiv v_{\rm obs} - v_{\rm flow}$ of the Coma cluster, where $v_{\rm obs}$ is the observed systematic velocity. The uncertainty in $v_{\rm flow}$ introduces an uncertainty of $\Delta\zeta_{\rm VII} = \pm0.013$ in ζ. The determination of the Hubble flow velocity also has a small dependence on the cosmological parameters $\Omega_{\rm m}$, Ω_Λ. However, at the distance of Coma this dependence is small enough that the resulting uncertainties can be neglected. Uncertainties in H_0 include the uncertainties III and V in Table 1, which introduce FP zeropoint uncertainties $\Delta\zeta_{\rm III} = \pm0.037$ and $\zeta_{\rm III} = \pm0.023$. The last systematic uncertainty that affects $\zeta_{\rm coma}$ stems from the fact that different authors get slightly different zeropoints, even if they assume exactly the same distance. Based on our own analysis of various literature sources, as well as the detailed analysis of Hudson et al. (2001), we estimate this systematic zeropoint uncertainty to be $\Delta\zeta_{\rm VIII} = \pm0.020$. Addition in quadrature of the uncertainties III, V, VII, and VIII yields a final systematic uncertainty in $\zeta_{\rm coma}$ of ±0.050. The FP zeropoint $\zeta_{\rm distant}$ of the intermediate-redshift cluster galaxy sample shares the systematic uncertainties III, V, and VIII with Coma. It also is subject to uncertainty I in Table 1 that results from uncertainties in $\Omega_{\rm m}$ and Ω_Λ, and uncertainty IV that results from cosmic variance in H_0. Addition in quadrature yields a final systematic uncertainty in $\zeta_{\rm distant}$ of ±0.049. To study M/L evolution we are now interested in the difference $\zeta_{\rm coma} - \zeta_{\rm distant}$. The uncertainties III, IV, and V in Table 3 drop out of this difference. However, the difference is subject to uncertainties I, VII and VIII. We include source VIII only once, because it was defined as a measure of the typical difference in zeropoint between different authors. There is also a new uncertainty due to cosmic variance in H_0 that is similar to source IV. However, the relevant scale is now the distance of the Coma cluster ($z = 0.025$), and not the scales $z \lesssim 0.1$ over which Type Ia supernovae have been used to calibrate H_0. Based on the discussion in Section 8.6 of Freedman et al. (2001) we estimate this systematic component to be less than 4%. This corresponds to a FP zeropoint difference $\Delta\zeta_{\rm IX} = \pm0.018$. Addition in quadrature yields a final systematic uncertainty in $\zeta_{\rm coma} - \zeta_{\rm distant}$ of ±0.030. Division by 0.83 yields the systematic uncertainty in $\delta\log(M/L)$ listed in equation (9).

The change with redshift implied by the FP zeropoint evolution listed in equation (9) is $\Delta \log(M/L)/\Delta z = \delta \log(M/L)/(\langle z \rangle_{\rm distant} - \langle z \rangle_{\rm local})$, which gives

$$\Delta \log(M/L)/\Delta z = -0.529 \pm 0.049\,({\rm random}) \pm 0.071\,({\rm systematic}) \quad (10)$$

This FP result agrees with that of vDvdM06, which found $\Delta \log(M/L)/\Delta z = -0.555 \pm 0.042$ (random) from a FP study of a larger sample of clusters that included the three clusters studied here.

The difference between the M/L evolution derived from the M/L–σ relation and dynamical modeling of internal kinematics, as reported in equation (6), and that derived from FP evolution, as reported in equation (10), is

$$[\Delta \log(M/L)_{\rm dyn} - \Delta \log(M/L)_{\rm FP}]/\Delta z = 0.072 \pm 0.067\,({\rm random}) \pm 0.097\,({\rm systematic}). \quad (11)$$

The listed random uncertainty is the quadrature sum of the random uncertainties in equations (6) and (10). This might be a slight overestimate, because it ignores possible correlations between the residuals from both methods. The listed systematic uncertainty is the quadrature sum of all those uncertainties that do not drop out of the difference under consideration. This includes the systematic uncertainties II, V, and VI in Table 1 and VII and VIII in Table 3. There also is a systematic uncertainty due to the cosmic variance in H_0 when measured on scales of $z \lesssim 0.025$ and $z \lesssim 0.1$, respectively. Based on the discussion in Section 8.6 of Freedman et al. (2001) we estimate this uncertainty to be $\Delta \log(M/L) = \pm 0.009$.

The upshot of equation (11) is that the M/L evolution derived here from detailed dynamical models is consistent with that derived from FP analysis of global parameters. The present paper therefore supports the conclusions drawn in vDvdM06 (and summarized in Section 1 of the present paper) about the star formation epoch of early type galaxies.

4. DEPENDENCE OF M/L EVOLUTION ON σ

Figure 3 shows the residuals with respect to the M/L–σ relation (i.e., with respect to the solid line in Figure 2b) for the sample of intermediate redshift cluster galaxies. The $\log(M/L)$ residuals do not show a significant correlation with $\log \sigma_{\rm eff}$. For example, the average residual for galaxies with $\sigma_{\rm eff} < 200\,{\rm km\,s^{-1}}$ is -0.010 ± 0.039, while the average residual for galaxies with $\sigma_{\rm eff} > 200\,{\rm km\,s^{-1}}$ is 0.008 ± 0.024. These values are consistent at the 1-σ level. This implies that the analysis yields the same evolution $\delta \log(M/L)$ (eq. [5]) independent of whether or not galaxies with low σ are excluded from the statistics. Phrased differently, there is no evidence for evolution of the slope of the M/L–σ relation out to $z \approx 0.5$. This can also be shown explicitly. A straight line fit to the data in Figure 2b yields slope $S = 1.117 \pm 0.113$, as compared to $S = 0.992 \pm 0.054$ for the sample of local galaxies in Figure 2a. Again, these values are consistent at the 1-σ level.

The relative constancy of the slope of the M/L–σ relation is consistent with some studies of FP evolution. For example, Kelson et al. (2000) find no statistically significant change in the tilt of the FP between the local Universe and a cluster at $z = 0.33$. However, many other FP studies, mostly towards higher redshifts, have recently found that the FP tilt does evolve (e.g., Wuyts et al. 2004; Treu et al. 2005a,b; van der Wel et al. 2004, 2005; di Serego Alighieri et al. 2005; and Jorgensen et al. 2006). In fact, we showed in vDvdM06 that the FP residuals for the same sample analyzed here show more evolution for galaxies with $\sigma \lesssim 200\,{\rm km\,s^{-1}}$ (or similarly, $M \lesssim 10^{11}\,{\rm M_\odot}$) than for galaxies with $\sigma \gtrsim 200\,{\rm km\,s^{-1}}$ (or similarly, $M \gtrsim 10^{11}\,{\rm M_\odot}$). Based on these results, the FP analysis in vDvdM06 was restricted to galaxies with $M > 10^{11}\,{\rm M_\odot}$. The same selection was applied in the derivation of equation (10). With this FP selection criterion, the inferred M/L evolution agrees with that derived from the dynamical models presented here (as quantified by eq. [11]). However, without this FP selection criterion the agreement is worse.

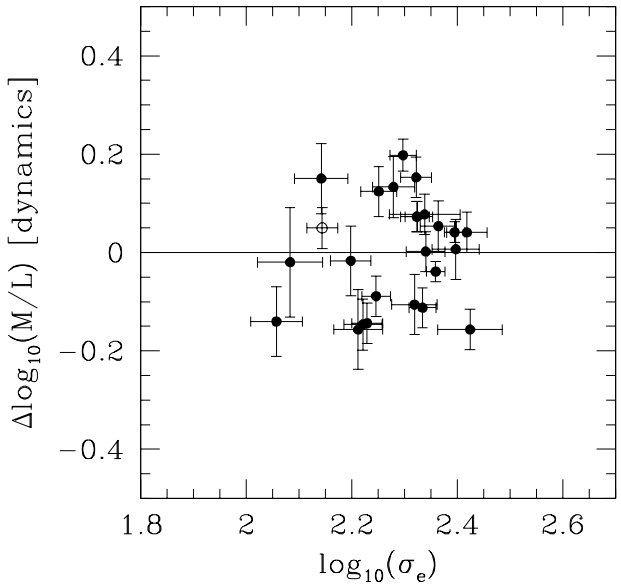

FIG. 3.— $\log(M/L)$ residuals with respect to the solid line in Figure 2b. There is no significant correlation with $\log \sigma_{\rm eff}$. So there is no evidence for evolution of the slope of the M/L–σ relation out to $z \approx 0.5$. Each datapoint is an individual galaxy in the sample of intermediate redshift cluster galaxies, with point types the same as in Figure 2.

This issue is further illustrated in Figure 4. It shows for each galaxy the difference between the evolution in $\log(M/L)$ inferred either from the dynamically inferred M/L–σ relation or from the FP. The differences are plotted as a function of $\log \sigma_{\rm eff}$. There is a clear trend with $\sigma_{\rm eff}$. The results from the two methods agree only when the comparison is restricted to galaxies with $\sigma \gtrsim 200\,{\rm km\,s^{-1}}$ (or similarly, $M \gtrsim 10^{11}\,{\rm M_\odot}$). It is shown by equation (11) that the difference between the two methods might be affected by various systematic uncertainties. However, these uncertainties are mostly related to uncertainties in distance scales. They cannot introduce a dependence on $\log \sigma_{\rm eff}$. Therefore, the trend in Figure 4 must have a different origin. We continue in the following subsections by exploring various possible explanations. This is an important issue, because differences in M/L evolution between low-mass and high-mass galaxies are generally interpreted as due to differences in stellar population age. Such age differences have a direct bearing on our understanding of galaxy formation.

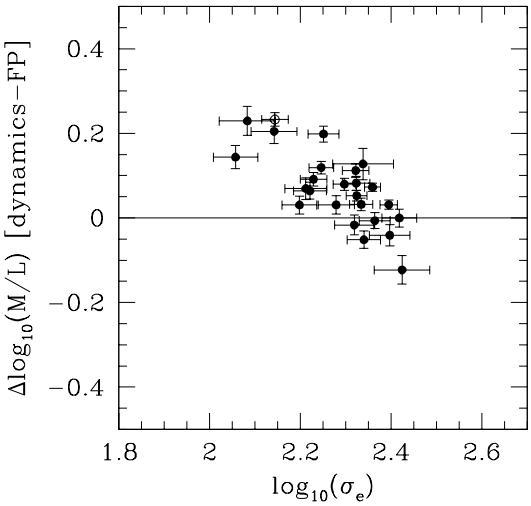

FIG. 4.— Difference between the evolution in $\log(M/L)$ as calculated either from dynamical models and the M/L–σ relation, or from the FP. The inferred evolution agrees for dispersions $\sigma_{\rm eff} \gtrsim 200\,{\rm km\,s^{-1}}$ (i.e., $\log\sigma_{\rm eff} \gtrsim 2.30$; or similarly, $M \gtrsim 10^{11}\,{\rm M}_\odot$). However, at lower dispersions the FP suggests more evolution than do the dynamical M/L measurements. Each datapoint is an individual galaxy in the sample of intermediate redshift cluster galaxies, with point types the same as in Figure 2.

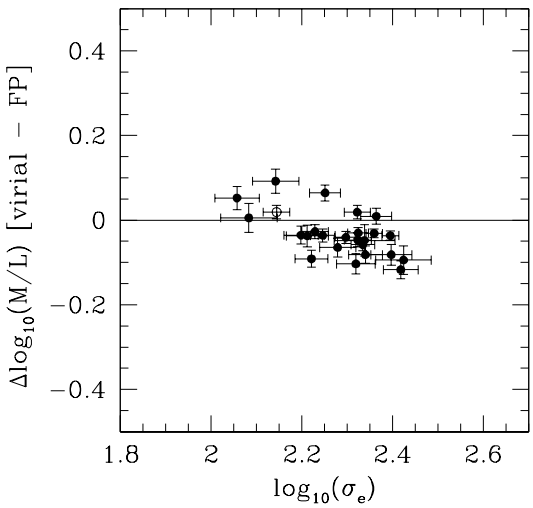

FIG. 5.— Difference between the evolution in $\log(M/L)$ as calculated either from the virial theorem and the M/L–σ relation, or from the FP. The two methods do not yield the same results, despite the fact that both analyses are based on exactly the same global properties ($\sigma_{\rm eff}$, $r_{\rm eff}$, and $I_{\rm eff}$) and use exactly the same local comparison sample (Coma). There is a trend with $\sigma_{\rm eff}$ in the same direction as in Figure 4. Each datapoint is an individual galaxy in the sample of intermediate redshift cluster galaxies, with point types the same as in Figure 2.

4.1. *Structure Evolution*

If galaxies do not change their structure over time then any evolution in either the FP or the M/L–σ relation must be due to M/L evolution. In this case, a study of the evolution of these two relations always implies the same (correct) M/L evolution. However, this equivalence ceases to exist when the structure of galaxies evolves with time.

As a simple illustration of the possible impact of structure evolution, consider the example in which some process changes the $r_{\rm eff}$ of a galaxy while M/L and $\sigma_{\rm eff}$ remain constant. This will obviously not move the galaxy with respect to the M/L–σ relation. However, the galaxy will move with respect to the FP. The virial theorem dictates that

$$(M/L)_{\rm vir} = K\sigma_{\rm eff}^2/(2\pi G r_{\rm eff} I_{\rm eff}), \qquad (12)$$

where G is the gravitational constant and K the structure constant, a scalar that depends on the structure of the galaxy (for example, a spherical model with a de Vaucouleurs $R^{1/4}$ surface brightness profile has $K = 5.95$). If we assume in this example that the galaxy changes its structure homologously, then K will remain constant. Equation (12) then implies that $\Delta\log I_{\rm eff} = -\Delta\log r_{\rm eff}$. Therefore, at its new $r_{\rm eff}$ the galaxy will be offset from the FP by an amount $\Delta\zeta = -0.17\Delta\log r_{\rm eff}$. The customary assumptions for interpreting FP evolution (see e.g., eq. [9]) would then incorrectly suggest a mass-to-light ratio evolution of $\Delta\log(M/L) = -0.20\Delta\log r_{\rm eff}$.

It is equally possible to construct examples in which FP evolution properly measures M/L evolution, whereas M/L–σ evolution does not. To illustrate this, consider the situation in which due to some process a galaxy homologously changes its $r_{\rm eff}$, $\sigma_{\rm eff}$ and $I_{\rm eff}$ while M/L remains constant. If $\Delta\log r_{\rm eff} = -2.71\Delta\log\sigma_{\rm eff}$ and $\Delta\log I_{\rm eff} = 4.71\Delta\log\sigma_{\rm eff}$, then the galaxy will continue to fall on the edge-on projection of the FP. The customary assumptions for interpreting FP evolution would then correctly suggest that there was no change in M/L. However, the galaxy will now be offset from the M/L–σ relation by an amount $\Delta\log(M/L) = 0.37\Delta\log r_{\rm eff}$.

These examples show that whenever there is evolution in any of the structural quantities $\sigma_{\rm eff}$, $r_{\rm eff}$, $\Sigma_{\rm eff} \equiv I_{\rm eff}(M/L)$, or K, then the M/L evolution inferred from the FP and from the M/L–σ relation will not generally agree with each other. One plausible explanation for the trend in Figure 4 is therefore that galaxies undergo structural evolution with time, and that this evolution is different for galaxies of low and high $\sigma_{\rm eff}$.

The assessment of the importance of this effect is complicated by the fact that our analysis of the evolution of the M/L–σ evolution has been based on rather different data than our analysis of the FP evolution. The former used spatially resolved brightness profiles and kinematics, whereas the latter used only the characteristic quantities $r_{\rm eff}$, $I_{\rm eff}$, and $\sigma_{\rm eff}$. A somewhat cleaner comparison can therefore be made through an analysis of M/L–σ evolution based on virial estimates from equation (12), which uses the same three characteristic quantities as FP studies. To this end, we first calculated the values of $(M/L)_{\rm vir}$ for the sample of Coma galaxies studied by Jorgensen et al. (1995a,b). The values thus obtained were fit by a straight line of the form given by equation (2) which yields parameters $Z_{\rm coma} = \log K + 0.163 \pm 0.015$ and $S_{\rm coma} = 0.887 \pm 0.095$. We then calculated $(M/L)_{\rm vir}$ for all of the intermediate-redshift cluster galaxies. The evolution for each galaxy was calculated by comparison to the $(M/L)_{\rm vir}$–σ relation for Coma.

Figure 5 shows for each galaxy the difference between the evolution thus determined and the evolution determined from the FP evolution. By contrast to Figure 4, both measures of evolution are now inferred entirely from the same global properties ($\sigma_{\rm eff}$, $r_{\rm eff}$, and $I_{\rm eff}$), and use exactly the same local comparison sample. However, there is a still a trend in the inferred M/L evolution with $\sigma_{\rm eff}$, in the same sense as in Figure 4. This sup-

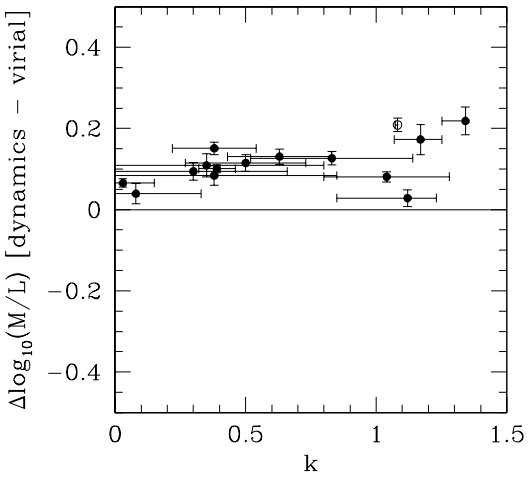

FIG. 6.— Difference between the evolution in $\log(M/L)$ as calculated from the M/L–σ relation using either dynamical models or the virial theorem. The difference is shown as a function of the rotation rate k determined in Paper I. For rapidly rotating galaxies the M/L evolution inferred from the dynamical models is less than that implied by the virial estimates. Each datapoint is an individual galaxy in the sample of intermediate redshift cluster galaxies, with point types the same as in Figure 2. Only those 15 galaxies are shown for which the rotation rate k could be reliably determined.

ports the view that structural quantities in addition to M/L are probably evolving with time. Note that it is not possible to identify whether a more accurate estimate of M/L evolution is obtained by studying FP evolution or M/L–σ evolution. For this one would need to know exactly how the structural properties of individual elliptical galaxies change with redshift, which is not well constrained observationally.

4.2. *Rotation*

The trend in Figure 5 is not as steep as that in Figure 4. This means that part of the trend in Figure 4 must be due to differences in evolution between our M/L values from dynamical modeling and the $(M/L)_{\rm vir}$ values determined from the virial theorem. Such differences are not necessarily unexpected, given that our models ought to be more accurate. They account for rotation and homological differences, between galaxies and as a function of redshift, whereas the virial analysis does not.

In Paper I we determined for each galaxy the normalized rotation measure k, which is similar to the quantity $(v/\sigma)^*$ that is often used for local galaxies. For $k = 0$ the galaxy is non-rotating, whereas for $|k| = 1$ the velocity dispersion tensor is isotropic and the galaxy is a so-called "oblate isotropic rotator". The quantity k is reasonably well determined for the 15 galaxies in the sample for which a slit was placed within 45° of the major axis, and which have projected ellipticity $\epsilon > 0.10$ (these galaxies are marked with an asterisk in Table 1 of Paper I). Figure 6 shows for these 15 galaxies the differences between the following two quantities: (a) the evolution inferred from our dynamical models and the local comparison sample described in Section 2; and (b) the evolution inferred from the $(M/L)_{\rm vir}$ estimates using Coma as comparison sample. Since both measures of evolution are based on an underlying relation between M/L and σ, any effects introduced by structure evolution, such as those described in Section 4.1, are now removed from the comparison. The differences thus calculated (which are equal to the the differences between the residuals shown in Figures 4 and 5) are shown as a function of the rotation parameter k. There is a significant trend for the residuals to be larger for galaxies that have more rotational support. For example, the quantity $\Delta\log(M/L)_{\rm dyn} - \Delta\log(M/L)_{\rm vir}$ has an average value of 0.095 ± 0.011 for galaxies with $k < 0.6$ and 0.138 ± 0.026 for galaxies with $k > 0.6$. By contrast, we have found no correlation with the observed axial ratio of each galaxy.

The dynamical models that we have used here explicitly account for the observed rotation of each galaxy, whereas studies based entirely on $\sigma_{\rm eff}$ do not. This causes $(M/L)_{\rm vir}$ or the FP to systematically underestimate the M/L of rapidly rotating galaxies. It is not immediately obvious though that the inferred M/L *evolution* would be impacted by this. Studies of FP evolution or $(M/L)_{\rm vir}$–σ evolution ignore rotation both in the local Universe and at intermediate redshift, so any bias might cancel out when different redshifts are compared. On the other hand, observations in the local universe generally use small apertures that cover only the central part of the galaxy, whereas observations of distant galaxies generally use apertures that cover most of the galaxy. To enable meaningful comparison, observations at different redshifts are generally transformed to a common aperture size using transformations that themselves do not explicitly account for rotation (e.g., Jorgensen et al. 1995b). Therefore, observations at different redshifts may be impacted by rotation in different manner. So any bias introduced through the neglect of rotation in FP or $(M/L)_{\rm vir}$ calculations may not cancel out when samples at different redshifts are compared. This may bias the inferred evolution and could therefore affect the trend in Figure 6. The fact that the trend in Figure 4 is steeper than that in Figure 5 is related to the fact that galaxies of low $\sigma_{\rm eff}$ tend to have more rotational support than those of high $\sigma_{\rm eff}$ (both in the local universe and in the sample of intermediate-redshift cluster galaxies, see Paper I).

Figure 6 shows that even at $k \approx 0$ there is a difference of ~ 0.05 dex between the evolution inferred from the dynamical and virial M/L estimates. The significance of this offset is low, given the systematic error quoted in equation (11). The offset could be due to (a combination of) several different effects. For example: (a) systematic uncertainties in the relative distance scale between our local comparison sample of Section 2 and Coma; (b) systematic errors in the conversions of observed velocity dispersions in some fixed aperture to $\sigma_{\rm eff}$; or (c) redshift evolution of the structure constant K.

On a separate note, we do not find a correlation between the residuals from the M/L–σ relation inferred from our dynamical models (i.e., the offset of the points in Figure 2b from the solid straight line in that figure) and either the rotation parameter k or the morphological types from Smail et al. (1997). This is shown in Figure 7. We discussed in Paper I that some of the most rapidly rotating galaxies in the sample could be misclassified S0 galaxies. Such galaxies, or other galaxies of intermediate and late Hubble types, might have recently transformed from star-forming field galaxies. If so, one would expect their M/L ratios to be smaller than for the true elliptical galaxies, which may have formed the bulk of their

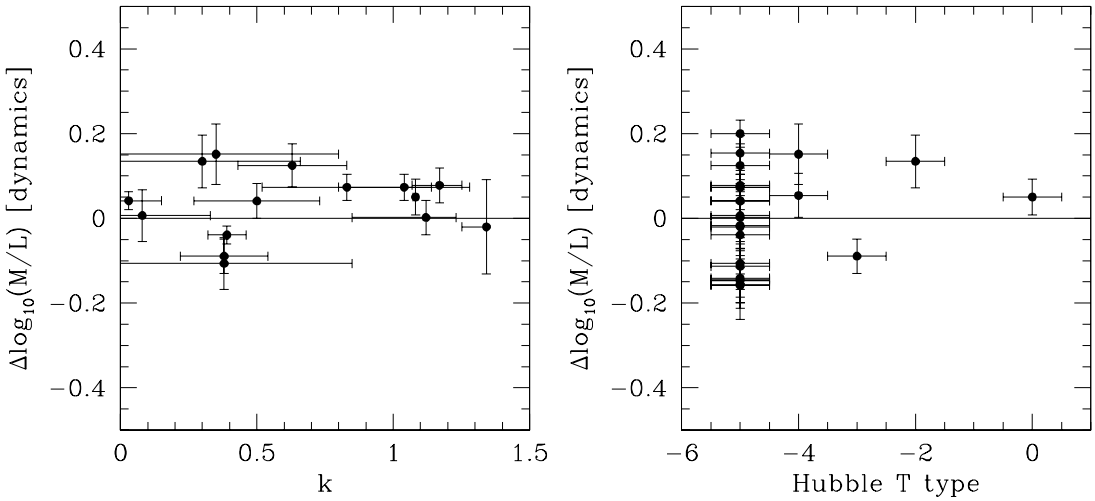

FIG. 7.— $\log(M/L)$ residuals for the intermediate redshift cluster galaxies with respect to the solid line in Figure 2b. (a) Residuals versus rotation rate k for the 15 galaxies with reliable k determinations. (b) Residuals versus Hubble T type from Smail et al. (1997) for the full sample; −5, −4, −3, −2, and 0 correspond to E, E/S0, S0/E, S0, and S0/Sa, respectively. There is no obvious trend in either panel that might have supported the view that more rapidly rotating or later-type galaxies formed the bulk of their stars more recently.

stars longer ago. Figure 7 shows no obvious trends that would support this view. However, a sample with a larger number of S0 and later-type galaxies would obviously be more suited to address this issue.

4.3. *Other Systematic Effects*

The slope of the M/L–σ relation does not change with redshift for our sample, despite the fact that the FP tilt does evolve with redshift. We have shown that this can be plausibly attributed to a combination of two effects: (a) evolution in structural properties; and (b) the neglect of rotational support in studies of FP evolution. Nonetheless, there are other systematic effects that may influence the comparison. In particular, it is worth considering potential systematic errors in the evolution inferred from our dynamical modeling approach. We discuss two possible effects, but conclude in the end that neither is likely to be a significant contributor to the trend seen in Figure 4.

4.3.1. *Environment*

It is possible that M/L depends not only on $\sigma_{\rm eff}$, but also on environment. Our sample of intermediate redshift galaxies consists of galaxies in rich cluster environments. To study M/L evolution one compares to local galaxies which generally reside in somewhat different environments. So any local dependence of M/L on environment would bias the inferred M/L evolution. If this is in fact an issue, then it is more likely to affect the evolution inferred from dynamical models and the M/L–σ relation, than it is to affect FP studies. The latter generally use Coma as a local comparison sample. While Coma is not as rich as clusters studied at higher redshift, it is nonetheless a dense cluster environment. By contrast, the local comparison sample used to construct the M/L–σ relation (Table 2) contains an inhomogeneous mixture of galaxies in cluster, group and field environments. It has been suggested that field galaxies might typically be younger, and thus have lower M/L values, than cluster galaxies (e.g., Diaferio et al. 2001; Bernardi et al. 2003; Annibali et al. 2006). If this were true, and in particular for galaxies of low σ or mass, then this might explain part of the trend seen in Figure 4. However, there is little evidence that any dependence on environment would in fact be larger for galaxies of low σ or mass (Clemens et al. 2006). Also, a significant fraction (25/60) of the galaxies in our local comparison sample (Table 2) come from the work of C06. They explicitly studied the residuals of the M/L–σ relation as a function of environment, and did not find any dependence.

To test directly for environmental effects we compared the M/L–σ relation for our local comparison sample to the $(M/L)_{\rm vir}$–σ relation for Coma. The zeropoint $Z_{\rm coma}$ and slope $S_{\rm coma}$ of the latter relation are listed in Section 4.1. The value of $S_{\rm coma}$ is consistent at the $\sim 1\sigma$ level with the slope $S = 0.992 \pm 0.054$ inferred for our local comparison sample. Also, the value of $Z_{\rm coma}$ is consistent with the value $Z = 0.896 \pm 0.010$ for the local comparison sample if $K = 5.40 \pm 0.23$. This value can be compared to the average $K = 5.09 \pm 0.19$ for the galaxies in our local comparison sample, which can be determined directly by equating the dynamical M/L to $(M/L)_{\rm vir}$ for these galaxies. These two estimates of K are entirely consistent, especially when taking into account the previously discussed systematic uncertainties in the relative distance scales between our local comparison sample and the Coma cluster. For comparison, C06 found that for data in the I-band $K \approx 4.8 \pm 0.1$. In addition to being a useful consistency check, these results show that there is no evidence for a strong environmental dependence of the M/L–σ relation in the local universe. The trend in Figure 4 therefore cannot be attributed to environmental influences on the analysis.

4.3.2. *Spatial Resolution*

FP and dynamical modeling analyses rely in different manner on knowledge of the galaxy surface brightness profile. To calculate the FP position of a galaxy one needs to know only the integrated luminosity within the effective radius. By contrast, to perform the dynamical modeling one needs to model the surface brightness profile down to very small radii, which requires accurate PSF deconvolution. Any systematic errors introduced by this are likely to produce a relative difference between M/L

evolution inferred from FP analysis and dynamical modeling. This is likely to affect low-mass galaxies, which are smaller on average, more than high-mass galaxies. So potential PSF deconvolution errors in our dynamical modeling could in principle produce a trend such as that in Figure 4. While this issue may be a contributing factor to the results in Figure 4, we do not believe that it can be the full explanation. The galaxies in our sample that provide evidence for evolution in the FP tilt have $r_{\rm eff}$ in the range $0.16''$–$0.80''$ (see fig. 5a of vDvdM06). Most of these galaxies are quite well resolved even with the $0.1''$ pixels of the HST/WFPC2. Nonetheless, future higher resolution imaging, such as now possible with the HST Advanced Camera for Surveys (ACS), would certainly decrease any sensitivity of the dynamical modeling on PSF deconvolution.

Even if limited spatial resolution were an issue for our models, it would not explain the entire trend in Figure 4. After all, a shallower trend is seen even in Figure 12, which does not involve any dynamical modeling at all. The hypothesis of errors due to limited spatial resolution could at best explain the trend in Figure 6. Galaxies with more rotational support tend to have lower mass (see Paper I), therefore tend to be smaller on average, and therefore could in principle be more affected by spatial resolution issues.

5. SUMMARY AND DISCUSSION

Many studies in the past decade have addressed the M/L evolution of early-type galaxies using the FP. This uses only global photometric and kinematic quantities and is therefore relatively straightforward to explore. However, FP evolution equals M/L evolution only if many simplifying assumptions are met, as discussed in Section 1. The validity of these assumptions has remained poorly verified. It is therefore important to address M/L evolution more directly by using dynamical models for spatially resolved photometric and kinematic data. In Paper I we constructed two-integral $f(E, L_z)$ models for 25 visually-classified early type (and in most cases elliptical) galaxies in the intermediate-redshift ($z \approx 0.5$) clusters CL3C295, CL0016+16 and CL1601+42. Fitting of the models to surface photometry from HST and kinematics from Keck/LRIS yielded for each galaxy the average rest-frame B-band M/L inside the spectroscopically explored region. The results allow a critical test of many of the assumptions that have underlied previous studies of FP evolution.

To study redshift evolution we needed a suitable comparison sample of M/L values for local early-type galaxies. We therefore compiled a sample of 60 galaxies in the local Universe for which detailed dynamical models were previously constructed to fit spatially resolved kinematical data. Attention was restricted to galaxies in five specific modeling studies that addressed large samples. All inferred M/L values were brought to a homogeneous distance scale, using distances obtained with the SBF method. Galaxies without SBF distances were excluded from the sample. All M/L values were transformed to the B band using either measured or estimated broad-band colors. C06 found that M/L correlates tightly with velocity dispersion, $\log(M/L) = Z + S\log(\sigma_{\rm eff}/[200\ {\rm km\,s^{-1}}])$, where $\sigma_{\rm eff}$ is the velocity dispersion inside an aperture of size equal to the effective radius $r_{\rm eff}$. This refined previous work which had found that M/L correlates (more loosely) with galaxy luminosity or mass. We confirm the finding of C06. Our larger, homogenized sample gives $Z = 0.896 \pm 0.010$ and $S = 0.992 \pm 0.054$. We estimate the systematic uncertainty in Z due to modeling uncertainties to be $\Delta Z = \pm 0.02$, based on a comparison of M/L results obtained from different dynamical modeling studies. The slope that we derive for the B band differs from the best-fit slope $S = 0.82 \pm 0.06$ found by C06 for the I band. This is due to the well-known fact that galaxies of low dispersion (or mass) tend to be bluer than those of high dispersion.

The M/L values inferred for the intermediate-redshift cluster sample follow a similar relation with $\sigma_{\rm eff}$ as found for the local galaxies. However, the zeropoint $Z = 0.657 \pm 0.022$ is smaller than for the local sample. The measured change of zeropoint with redshift implies that $\Delta\log(M/L)/\Delta z = -0.457 \pm 0.046\,({\rm random}) \pm 0.078\,({\rm systematic})$. A comparison of the FP defined by the high-mass galaxies with $M \gtrsim 10^{11}\ {\rm M}_\odot$ in the same sample with that measured for the nearby Coma cluster yields $\Delta\log(M/L)/\Delta z = -0.529 \pm 0.049\,({\rm random}) \pm 0.071\,({\rm systematic})$. The systematic uncertainties in these results are dominated by a variety of issues that affect our knowledge of the relative distance scale between local and distant galaxies. Although these systematic uncertainties are often not explicitly addressed, we stress that they are present in all studies of M/L evolution that use either dynamical models or the FP. The results from both methods are consistent with passive evolution of high-mass galaxies following formation at high redshift, as quantified in vDvdM06.

Comparison of the M/L evolution inferred from our dynamical modeling study and from the FP yields excellent agreement for massive galaxies. This is an important *a posteriori* verification of the assumptions that have underlied all previous FP evolution studies. It shows that to lowest order FP evolution does indeed measure M/L evolution, as suggested also by the results of Treu & Koopmans (2004) for lensing galaxies. It also shows that the subset of hierarchical structure formation models in which FP zeropoint evolution does not track M/L evolution (e.g., Almeida et al. 2006) is inconsistent with our observational understanding of early-type galaxies. Our results provide no evidence that the galaxies in the sample with the latest Hubble types (i.e., E/S0, S0/E, S0, or S0/Sb) or the galaxies with the highest rotation rates tend to have lower M/L values. This might have been expected if such galaxies transformed recently from star-forming field galaxies.

While there is broad agreement between the dynamical modeling and the FP results, we find important differences in the behavior of M/L evolution as a function of $\sigma_{\rm eff}$ (or similarly, mass). For the dynamically inferred M/L–σ relation we find no evidence for a change of the slope with redshift, and therefore no dependence of M/L evolution on $\sigma_{\rm eff}$. By contrast, our own work for this same sample and that of many previous authors on other samples has found that the FP tilt does evolve with redshift. We studied this difference by analyzing the residuals with respect to the fitted relations, and by considering also the evolution implied by $(M/L)_{\rm vir}$ estimates from the virial theorem. Based on this, we find that the

difference between the results from FP evolution and dynamically determined M/L–σ evolution can be plausibly attributed to a combination of two effects: (a) evolution in structural properties; and (b) the neglect of rotational support in studies of FP evolution. We investigated other potential explanations as well, including the possibility that our results may be biased due to unaccounted local dependencies of M/L on environment, or the possibility that systematic errors may affect our results for the smallest galaxies due to the finite spatial resolution of the HST imaging data. However, we argue that neither of these latter issues significantly affects our analysis.

Both FP evolution and evolution of the M/L–σ relation constrain the M/L evolution of elliptical galaxies. However, these approaches need not give the same answer (or more generally, the correct answer) if the structure of galaxies evolves with time. We find some evidence for this from the fact that the results from FP evolution and $(M/L)_{\rm vir}$–σ evolution differ (in the sense that there is a slight trend with $\sigma_{\rm eff}$), even when the analysis is in both cases based on exactly the same global properties ($\sigma_{\rm eff}$, $r_{\rm eff}$, and $I_{\rm eff}$) and uses exactly the same local comparison sample (Coma). In general, neither FP evolution nor evolution of the M/L–σ relation can uniquely and correctly determine the amount of M/L evolution, unless one knows (or correctly assumes) how the structural properties of the galaxies change with time. This is is not very well constrained observationally and one therefore has to rely on assumptions and theoretical insights. Translation of M/L–σ evolution into M/L evolution assumes only that the $\sigma_{\rm eff}$ of galaxies does not change over time. By contrast, translation of FP evolution into M/L evolution assumes that none of the quantities $\sigma_{\rm eff}$, $r_{\rm eff}$, $\Sigma_{\rm eff} \equiv I_{\rm eff}(M/L)$, or the structure constant K change over time. Although elliptical galaxies are collisionless systems, all these structural quantities can in fact change through mergers. However, the inferred M/L evolution is in practice used primarily to estimate the mean age of the stars under the assumption that only the luminosity is evolving (e.g., vDvdM06). This relaxes the underlying assumptions in the sense that the correct age is obtained (but not the correct M/L evolution) as long as any evolution of structural parameters moves galaxies only along the M/L–σ relation or along the edge-on projection of the FP. Models have suggested that structural changes induced by mergers do indeed approximately have this property (Gonzalez-Garcia & van Albada 2003; Boylan-Kolchin, Ma, & Quataert 2006; Robertson et al. 2006).

An approach that is based on dynamical models has less built-in assumptions than approaches (such as those using the FP or $(M/L)_{\rm vir}$ values) that are based entirely on global or characteristic quantities. In particular, the M/L values that we determined in Paper I account for several known non-homologies between galaxies, such as differences in axial ratio, brightness profile, rotational support, and internal velocity distribution. Moreover, kinematical profiles as a function of radius were calculated and fitted, instead of just a single characteristic dispersion. We found that the difference in the M/L evolution inferred from either dynamical models or the virial theorem correlates with the galaxy rotation rate k. This suggests that the omission of rotation in studies of FP evolution may be an important oversimplification. Nonetheless, it is important to stress that many caveats remain even with the dynamical modeling approach explored here. For example, if the triaxiality or velocity dispersion anisotropy of early-type galaxies evolves with redshift then this might bias the results of our dynamical models (as it would for FP studies). Also, both FP studies and the present work may suffer from "progenitor bias". This is the bias introduced by the fact that some of today's early-type galaxies may not be identified as early-type galaxies in samples at higher redshifts (see vDvdM06 for a discussion of the size of this bias).

In vDvdM06 we reported a steeping of the FP tilt with redshift for our sample galaxies. This is generally interpreted to mean that low-mass galaxies have undergone more M/L evolution than high-mass galaxies, and are therefore younger. However, the results presented here show that this conclusion need not necessarily be correct: the dynamical models provide little evidence for a difference in M/L evolution between low-mass and high-mass galaxies; and the steepening of the FP tilt may be affected by other issues than M/L evolution. This does not rule out the possibility that low-mass galaxies have younger population ages than high-mass galaxies. But it does mean than one should be careful in drawing conclusions of this nature entirely on the basis of FP data. In general it is important to test for differences in population age also on the basis of other considerations. For example, van der Wel et al. (2005) and Treu et al. (2005b) considered broad-band colors and spectroscopic diagnostics in combination with FP residuals to argue for age differences between field galaxies of different mass. Their results are not necessarily inconsistent with those presented here, because the situation may be different for galaxies in the field and in clusters and it may be different at different redshifts.

Our work shows that dynamical modeling of large samples of galaxies at intermediate redshifts provides a powerful new method for the study of galaxy evolution. It therefore seems useful to expand the present work to other samples that explore a wider range of redshifts, environments, and galaxy types.

We thank Michele Cappellari, Arjen van der Wel and Marijn Franx for useful discussions and suggestions. Part of this research was carried out at the Kavli Institute for Theoretical Physics in Santa Barbara, supported in part by the National Science Foundation under Grant No. PHY99-07949.

REFERENCES

Almeida, C., Baugh, C. M., & Lacey, C. G. 2006, MNRAS, submitted [astro-ph/0608544]
Annibali, F., Bressan, A., Rampazzo, R., Danese, L., & Zeilinger, W. W. 2006, A&A, in press [astro-ph/0609175]
Bell, E. F., & de Jong, R. S. 2001, ApJ, 550, 212
Bernardi, M., et al. 2003, AJ, 125, 1866
Binney, J. J., & Merrifield, M. 1998, Galactic Astronomy (Princeton: Princeton University Press)
Boylan-Kolchin, M., Ma, C.-P., & Quataert, E. 2006, MNRAS, 369, 1081
Bruzual, G, & Charlot, S. 2003, MNRAS, 344, 1000
Cappellari, M., et al. 2006a, MNRAS, 366, 1126 (C06)

Clemens, M. S., Bessan, A., Nikolic, B., Alexander, P., Annibali, F., Rampazzo, R. 2006, MNRAS, 2006, 370, 702
Colless, M., Saglia, R. P., Burstein, D., Davies, R. L., McMahan R. K., Wegner, G. 2001, MNRAS, 321, 277
Courteau, S., & Rix, H.-W. 1999, ApJ, 513, 561
Davis, L. E., Cawson, M., Davies, R. L., & Illingworth, G. 1985, AJ, 90, 169
De Lucia, G., Springel, V., White, S. D. M., Croton, D., & Kauffman, G. 2006, MNRAS, 366, 499
de Vaucouleurs, G., de Vaucouleurs, A., Corwin, H. G., Buta, R. J., Paturel, G., & Fouque, P. 1991, Third Reference Catalogue of Bright Galaxies (New York: Springer) (RC3)
Diaferio, A., Kauffmann, G., Balogh, M. L., White, S. D. M., Schade, D., & Ellingson, E. 2001, MNRAS, 323, 999
di Serego Alighieri, S., et al. 2005, A&A, 442, 125
Djorgovski, S., & Davis, M. 1987, ApJ, 313, 59
Dressler, A. 1980, ApJ, 236, 351
Dressler, A., Lynden-Bell, D., Burstein, D., Davies, R. L., Faber, S. M., Terlevich, R., Wegner, G. 1987, ApJ, 313, 42
Dressler, A., & Gunn, J. E. 1992, ApJS, 78, 1
Dressler, A., et al. 1997, ApJ, 490, 577
Dressler, A., Smail, I., Poggianti, B. M., Butcher, H., Couch, W. J., Ellis, R. S., Oemler, A. Jr. 1999, ApJS, 122, 51
Faber, S.M., Wegner, G., Burstein, D., Davies, R. L., Dressler, A., Lynden-Bell, D., & Terlevich, R. J. 1989, ApJS, 69, 763 (F89)
Ferrarese, L., et al. 2000, ApJ, 529, 745
Freedman, W. L., et al. 2001, ApJ, 553, 47
Gebhardt, K., et al. 2003, ApJ, 583, 92 (G03)
Gonzalez-Garcia, A. C., & van Albada, T. S. 2003, MNRAS, 342, L36
Hudson, M. J., Lucey, J. R., Smith, R. J., Schlegel, D. J., & Davies, R. L. 2001, 327, 265
Jensen, J. B., Tonry, J. L., Barris, B. J., Thompson, R. I., Liu, M. C., Rieke, M. J., Ajhar, E. A., & Blakeslee, J P. 2003, ApJ, 583, 712
Jorgensen, I., Franx, M., & Kjaergaard, P. 1995a, MNRAS, 273, 1097
Jorgensen, I., Franx, M., & Kjaergaard, P. 1995b, MNRAS, 276, 1341
Jorgensen, I., Chiboucas, K., Flint, K., Bergmann, M., Barr, J., Davies, R. L. 2006, ApJ, 639, L9
Kelson, D. D., Illingworth, G. D., van Dokkum, P. G., & Franx, M. 2000, ApJ, 531, 184
Kronawitter, A., Saglia, R. P., Gerhard, O., & Bender, R. 2000, A&AS, 144, 53 (K00)
Lauer, T., et al. 2005, AJ, 129, 2138
Magorrian, J., et al. 1998, AJ, 115, 2285 (M98)
Mei, S., et al. 2005, ApJ, 625, 121
Moran, S. M., Ellis, R. S., Treu, T., Smail, I., Dressler, A., Coil, A. L., & Smith, G. P. 2005, ApJ, 634, 977
Nagamine, K., Cen, R., Hernquist, L., Ostriker, J. P., Springel, V. 2005, ApJ, 627, 608
Peletier, R. F., Davies, R. L., Illingworth, G. D., Davis, L. E., & Cawson, M. 1990, AJ, 100, 1091
Persic, M., Salucci, P., & Stel, F. 1996, MNRAS, 281, 27
Press, W. H., Teukolsky, S. A., Vetterling, W. T., & Flannery, B. P. 1992, Numerical Recipes (Cambridge: Cambridge University Press)
Robertson, B., Cox, T. J., Hernquist, L., Franx, M., Hopkins, P. F., Martini, P., Springel, V. 2006, ApJ, 641, 21
Sakai, S., Ferrarese, L., Kennicutt, R. C. Jr., & Saha, A. 2004, ApJ, 608, 42
Smail, I., Dressler, A., Couch, W. J., Ellis, R. S., Oemler, A., Jr., Butcher, H., Sharples, R. M. 1997, ApJS, 110, 213
Smith, R. J., Lucey, J. R., & Hudson, M. J. 2006, MNRAS, submitted
Spergel, D. N., et al. 2003, ApJS, 148, 175
Tonry, J. L., Blakeslee, J P., Ajhar, E. A., & Dressler, A. 2000, ApJ, 530, 625
Tonry, J. L., Dressler, A., Blakeslee, J P., Ajhar, E. A., Fletcher, A. B., Luppino, G. A., Metzger, M. R., & Moore, C. B. 2001, ApJ, 546, 681 (T01)
Tremaine, S., et al. 2002, ApJ, 574, 740
Treu, T., & Koopmans, L. V. E. 2004, ApJ, 611, 739
Treu, T., Ellis, R. S., Liao, T. X., & van Dokkum, P. G. 2005a, ApJ, 622, L5
Treu, T., et al. 2005b, ApJ, 633, 174
van Albada, T. S., Bahcall, J. N., Begeman, K., & Sancisi, R. 1985, ApJ, 295, 305
van der Marel, R. P. 1991, MNRAS, 248, 515 (vdM91)
van der Marel, R. P., & van Dokkum, P. G. 2006, ApJ, submitted (Paper I)
van der Wel, A., Franx, M., van Dokkum, P. G., & Rix, H.-W. 2004, ApJ, 601, L5
van der Wel, A., Franx, M., van Dokkum, P. G., Rix, H.-W., Illingworth, G. D., & Rosati, P. 2005, ApJ, 631, 145
van Dokkum, P. G., & Franx, M. 1996, MNRAS, 281, 985
van Dokkum, P. G., Franx, M., Kelson, D. D., & Illingworth, G. D. 1998, ApJ, 504, L17
van Dokkum, P. G., & van der Marel, R. P. 2006, ApJ, in press (vDvdM06) [astro-ph/0609587]
Woo, J.-H., Urry, C. M., Lira, P., van der Marel, R. P., & Maza, J. 2004, ApJ, 617, 903
Wuyts, S., van Dokkum, P. G., Kelson, D. D., Franx, M., & Illingworth, G. D. 2004, ApJ, 605, 677